Current Biology 16, 166–172, January 24, 2006 ©2006 Elsevier Ltd All rights reserved DOI 10.1016/j.cub.2005.11.071

Report

Comparison of Gene Expression in Male and Female Mouse Blastocysts Revealed Imprinting of the X-Linked Gene, *Rhox5/Pem*, at Preimplantation Stages

Shin Kobayashi,[1] Ayako Isotani,[1,2] Nathan Mise,[3] Masamichi Yamamoto,[4] Yoshitaka Fujihara,[1,5] Kazuhiro Kaseda,[1] Tomoko Nakanishi,[1,6] Masahito Ikawa,[1] Hiroshi Hamada,[4] Kuniya Abe,[3] and Masaru Okabe[1,2,5,*]

[1] Research Institute for Microbial Diseases
Osaka University
3-1 Yamadaoka
Suita, Osaka 565-0871
Japan

[2] Graduate School of Pharmaceutical Sciences
Osaka University
1-6 Yamadaoka
Suita, Osaka 565-0871
Japan

[3] Technology and Development Team for Mammalian Cellular Dynamics
BioResource Center
RIKEN Tsukuba Institute
3-1-1 Koyadai
Tsukuba Ibaraki 305-0074
Japan

[4] Developmental Genetics Group
Graduate School of Frontier Biosciences
Osaka University
1-3 Yamadaoka
Suita, Osaka 565-0871
Japan

[5] Graduate School of Medicine
Osaka University
2-2 Yamadaoka
Suita, Osaka 565-0871
Japan

Summary

Mammalian male preimplantation embryos develop more quickly than females [1, 2]. Using enhanced green fluorescent protein (EGFP)-tagged X chromosomes to identify the sex of the embryos, we compared gene expression patterns between male and female mouse blastocysts by DNA microarray. We detected nearly 600 genes with statistically significant sex-linked expression; most differed by 2-fold or less. Of 11 genes showing greater than 2.5-fold differences, four were expressed exclusively or nearly exclusively sex dependently. Two genes (*Dby* and *Eif2s3y*) were mapped to the Y chromosome and were expressed in male blastocysts. The remaining two (*Rhox5/Pem* and *Xist*) were mapped to the X chromosome and were predominantly expressed in female blastocysts. Moreover, *Rhox5/Pem* was expressed predominantly from the paternally inherited X chromosome, indicating sex differences in early epigenetic gene regulation.

*Correspondence: okabe@gen-info.osaka-u.ac.jp
[6] Present address: Institute of Applied Biochemistry, University of Tsukuba, Tsukuba Science City, Ibaraki 305-8572, Japan.

Results

Sex-Linked Differential Gene Expression

In mammals, phenotypic gender is normally determined at the time of gonadal differentiation [3]. However, this may not be the sole determinant. For example, male blastocysts develop more quickly than female blastocysts [1, 2], and expression of several genes, such as murine *Xist* [4, 5], bovine *G6PD* [6, 7], *ZFX* [7], *HPRT* [6] and *INF-t* [8], and murine *Zfy* and *Sry* [9], is different in each sex. However, there is no report on global differences in gene expression in male and female blastocysts, largely because of the technical difficulty in sexing many blastocysts quickly and accurately. We overcame this by using a transgenic mouse line in which the X chromosome is tagged with a ubiquitously-expressed EGFP transgene (X^{GFP}) [10–12]. The system is shown in Figures 1A and 1B. Transgenic males ($X^{GFP}Y$) were mated with wild-type females (XX). Only the female embryos (XX^{GFP}) fluoresce green because of the paternally inherited X^{GFP}.

More than 1000 sexed blastocysts were studied. The global gene-expression patterns of male and female blastocysts were compared with the Agilent Mouse Development DNA microarray, which contains 20,371 transcripts (http://lgsun.grc.nia.nih.gov/cDNA/cDNA.html). Three independent experiments were carried out, and Figure 1C shows the normalized results. We identified 591 differentially expressed genes (blue spots); three hundred and eleven were expressed to a higher degree in female blastocysts ($p < 0.01$), and 280 were expressed to a higher degree in males ($p < 0.01$). Most of the differences were 2-fold (200%) or less (Figure 1C).

Of seven genes previously reported to be expressed differentially in male and female blastocysts of the cow and mouse [4–9], three were not represented in this microarray and one was not expressed in the mouse, leaving three candidate genes (*Xist, G6pd, and Hprt*) available for analysis. These were all significantly differently expressed by sex and are listed in Table 1.

Genes showing more than a 2.5-fold (250%) difference in expression (indicated by numbers in Figure 1C and Tables 1 and 2) were reexamined for their expression by reverse transcriptase polymerase chain reaction (RT–PCR) with blastocysts sexed by X^{GFP}. Of these, *Xist* and *Rhox5/Pem* on the X chromosome were predominantly expressed in females, whereas *Dby* and *Eif2s3y* on the Y chromosome were exclusively expressed in males (Figure 2). The same results were obtained with wild-type blastocysts not expressing EGFP (Figure S1 in the Supplemental Data available with this article online).

Verification of Imprinting of the *Rhox5/Pem* Gene

Because *Rhox5/Pem* is located on the X chromosome and is predominantly expressed in females, we

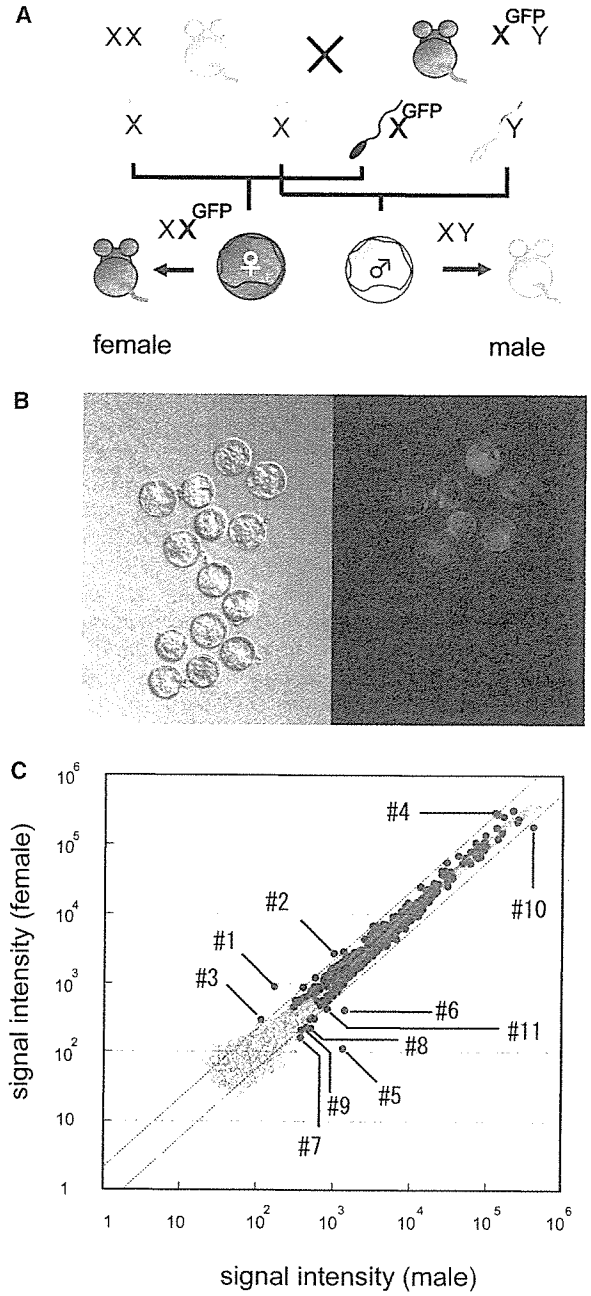

Figure 1. Screening of Differentially Expressed Genes between Sexes at the Preimplantation Stage

(A) The scheme of a X^{GFP} sexing system.

(B) Blastocysts at 3.5 dpc. Only female embryos become green. (Left: bright field. Right: dark field).

(C) Expression profiling of 20K genes between nonfluorescent male and fluorescent female blastocysts. For each gene, average signal intensity is displayed on a scatter plot. Genes that showed significantly different expression levels between females and males at the 1% significance level ($p < 0.01$; the complete description of the statistical methods is available in the technology section of the Rosetta Biosoftware website, http://www.rosettabio.com/tech/default.htm) are displayed as blue spots, and the others are displayed as gray spots. The numbered genes were re-examined for their expression by RT–PCR. Dotted lines indicate 2.0-fold (200%) expression differences.

examined whether it is imprinted, like the *Xist* gene [4, 5]. To distinguish paternal from maternal expression, we produced inter-subspecific F1 mice by crossing *M. m. musculus* (C57BL/6;B6) with *M. m. molossinus* (JF1/Ms;JF1). A DNA polymorphism in the 3′-UTR of the *Rhox5/Pem* gene (Figure 3A) is detectable by restriction fragment length polymorphism (RFLP) analysis with BsrBI. This was used to analyze the active allele in F1 blastocysts derived from mating between C57BL/6 females and JF1/Ms males (B6 × JF1) and the reciprocal cross of JF1/Ms females with C57BL/6 males (JF1 × B6). The RT-PCR products (Figure 3B) clearly show that the gene was predominantly expressed from the paternally inherited X chromosome.

Because early preimplantation-stage embryos already show dosage compensation via inactivation of the paternal X chromosome (Xp) [13–15], we examined whether there was expression of the paternal allele of *Rhox5/Pem* from the 2 cell stage to the blastocyst in embryos from the *M. m. musculus* × *M. m. molossinus* crosses. Figure 3C shows that the gene was expressed predominantly from Xp after the 8 cell stage to the blastocyst stage. This indicated that *Rhox5/Pem* escaped Xp inactivation.

Rhox5/Pem expression levels in male and female post-implantation stages were also examined in embryos at 5.5, 6.5, and 7.5 days post-coitum (dpc) by whole-mount in situ hybridization (Figure 4). Despite the predominant expression in female blastocysts, *Rhox5/Pem* was expressed in both male and female later-stage embryos: not in the epiblasts, but in extraembryonic ectoderm (ExE) and visceral endoderm (VE). When the expressed allele was examined in inter-subspecific crosses, *Rhox5/Pem* was expressed predominantly as the maternal allele in the 7.5 dpc embryos (Figure 3C, right panel).

Discussion

In eutherian mammals, male preimplantation embryos develop more rapidly than females in a number of species, such as the mouse [1, 2], cow [16, 17], human [18], sheep [19], and pig [20]. These differences precede gonadal sex commitment. Here we found minor but statistically significant sex differences in the expressions of nearly 600 genes. These may have arisen from slight differences in developmental stages between the male and female blastocysts, so we cannot conclude that all are associated with sex differentiation. However, we have demonstrated here that at least four genes are certainly expressed differently, not by stage but by sex. We presume that the actual number of genes involved in such sex differences is likely to exceed the small number of previously reported genes [4–9].

Figure 5 indicates the chromosomal distribution of the genes that are differentially expressed by sex. There was no obvious tendency in the distribution of male upregulated genes, whereas there were apparently more female upregulated genes on the X chromosome. When we plotted 212 of these X-linked genes on the X chromosome, most of the variance in expression remained within the range of $1 \leq FC \leq 2$ (Figure S2). These included previously reported female upregulated genes such as *G6pd* and *Hprt* (Table 1, lower row). This slight differential

Table 1. Upregulated Genes in Female Blastocysts

Number[a]	Gene Name	Accession Number	Map Position	N-Fold Change	*p* Value	Intensity (Male)	Intensity (Female)
1	*Xist*[b]	K0418D06-3	X	2.8	4.9×10^{-6}	242	841
2	*Rhox5/Pem*	G0109E12-3	X	2.6	6.3×10^{-28}	1323	3372
3	*EST*	J0030A03-3	X	2.6	4.4×10^{-3}	133	320
4	*EST*	H3075D02-3	8	2.5	4.6×10^{-12}	161060	399351
	G6pd[b]	G0120A12-3	X	1.2	1.5×10^{-3}	2412	2801
	Hprt[b]	H3152G02-3	X	1.5	2.0×10^{-33}	3255	5038

All genes showing more than a 2.5-fold (250%) change in expression level are listed in the upper part of the table.
[a] Numbers correspond to those indicated in Figure 1C.
[b] Genes that were previously reported to be differently expressed.

Table 2. Upregulated Genes in Male Blastocysts

Number[a]	Gene Name	Accession Number	Map Position	N-Fold Change	*p* Value	Intensity (Male)	Intensity (Female)
5	*Dby*	L0814A11-3	Y	−14.8	0	1593	106
6	*Eif2s3y*	H3079H10-3	Y	−3.9	5.0×10^{-26}	1680	460
7	*1110038H03Rik*	C0508G12-3	12	−3.2	7.2×10^{-3}	428	185
8	*EST*	C0282H03-3	17	−3.1	6.0×10^{-4}	584	254
9	*1700019B01Rik*	J0408D11-3	7	−2.7	6.5×10^{-3}	514	259
10	*2310061F22Rik*	J0041H02-3	8	−2.7	1.1×10^{-13}	579807	212643
11	*EST*	L0864B07-3	3	−2.5	4.2×10^{-3}	984	478

All genes for which the change in expression level is less than −2.5-fold are listed.
[a] Numbers correspond to those indicated in Figure 1C.

expression of many X-linked genes may be attributable to incomplete X inactivation or to the reactivation of X-linked genes in epiblast cells.

Many of the genes showing differential expression between sexes were linked to the X chromosome, but only two genes were linked to the Y chromosome. More are likely to be present because some Y-linked genes (*Sry* and *Zfy*) that are expressed in blastocysts were not on our microarray. Other known Y-linked genes on the array are listed in Table S1. However, we clearly detected differential expression of *Dby* and *Eif2s3y*. Because the Y chromosome may accelerate growth of preimplantation mouse embryos, whereas paternally derived X chromosomes or double X chromosomes retard it [21–24], our findings may help elucidate these phenomena.

As with the *Xist* gene, *Rhox5/Pem* was predominantly expressed from the paternally derived X chromosome in the blastocyst. This is a member of a homeobox gene cluster that is mainly expressed in reproductive tissues such as those of the testis, ovary, and placenta, which may play a role in controlling the development of these organs [25]. At present we have no information on the mechanism that enables preferential expression of the paternal *Rhox5/Pem* allele from the 8 cell to the blastocyst stage, when the paternal X is thought to be inactivated, or how the subsequent switch to expression of the maternal allele is brought about. Further experiments are needed to address these issues. However it is known that some imprinted genes show complicated expression patterns. One example is mouse *Grb10*, which shows paternal expression in the brain and maternal expression in other tissues [26, 27]. It is not clear if this imprinting of *Rhox5/Pem* disappeared after implantation, but the expression pattern shown in Figure 3C suggests stage-specific imprinting of this gene.

Using gene targeting, MacLean et al. showed that *Rhox5/Pem* null males were subfertile with reduced sperm count and decreased sperm motility [25]. However, they did not report the effect of gene disruption on embryonic development. It would be worthwhile to examine the early embryonic development between male- and female-targeted mice. However, *Rhox5* is part

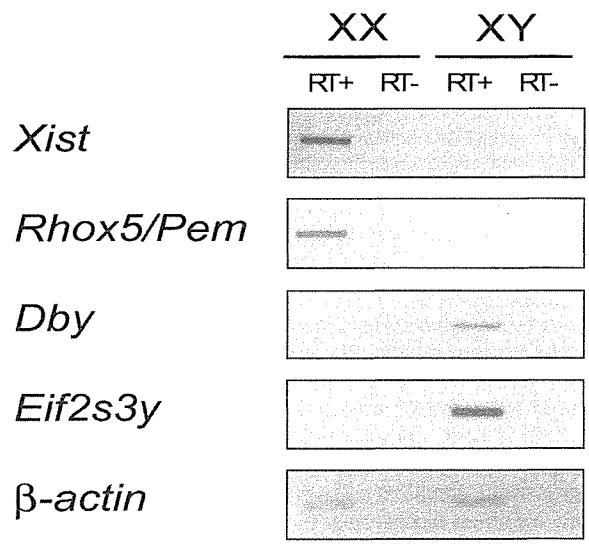

Figure 2. RT-PCR Analysis of Differentially Expressed Genes

Genes showing expression differences of more than 2.5-fold (250%) (see Tables 1 and 2) were chosen, and RT–PCR allowed the differential expression of the genes to be re-examined. Among these genes, four (*Xist, Rhox5/Pem, Dby,* and *Eif2s3y*) showed obvious differences. It should be noted that very weak expression of *Xist* and *Rhox5/Pem* was detected in male blastocysts when additional PCR cycles were carried out.

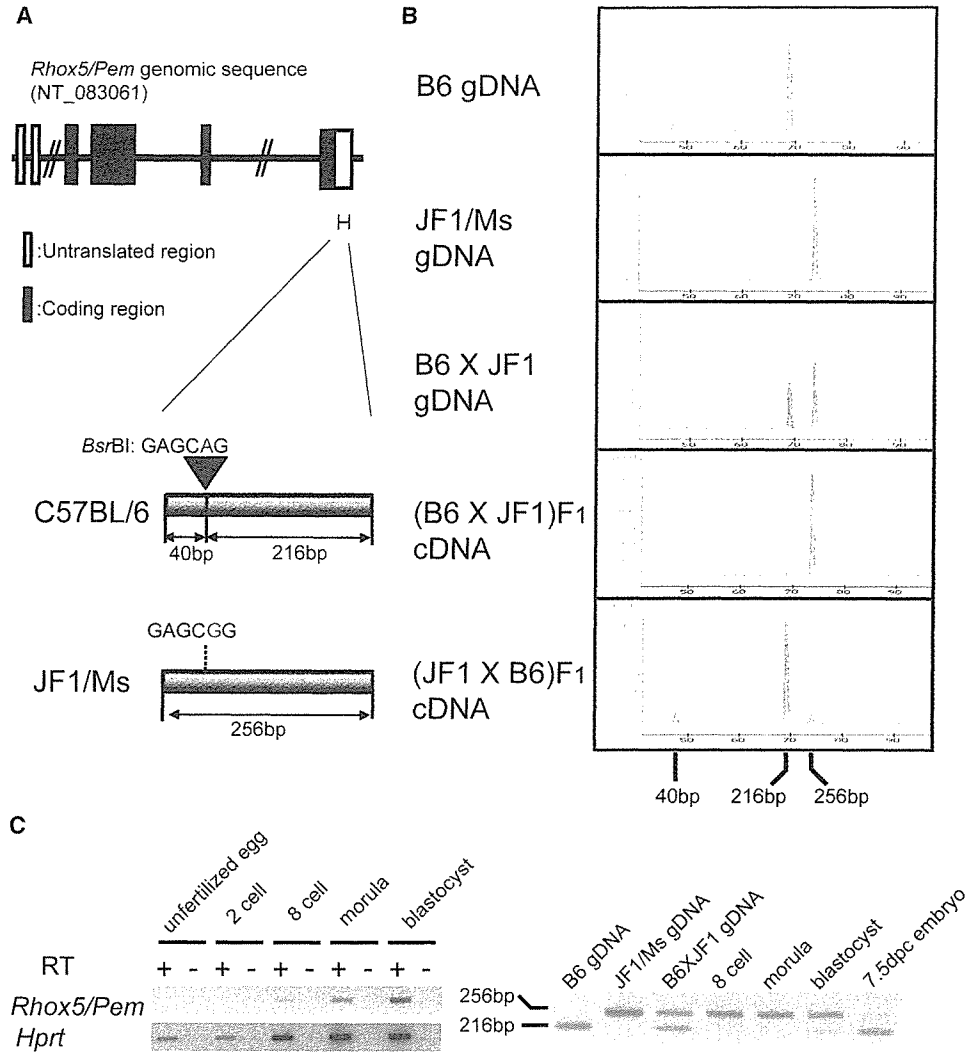

Figure 3. Verification of the *Rhox5/Pem* Gene Imprinting

(A) The single-nucleotide polymorphism detected in C57BL/6;B6 (*M. m. musculus*) and JF1/Ms;JF1 (*M. m. molossinus*) is shown. The BsrBI site (GAGCAG) in the B6 allele was changed to GAGCGG in the JF1 allele. These alleles could be distinguished by digestion with BsrBI; 40 bp and 216 bp digested PCR fragments appeared in the B6 sample, whereas a 256 bp undigested PCR product was seen in the JF1/Ms samples.

(B) Predominant expression of *Rhox5/Pem* from paternal X chromosome was determined by RT-PCR and RFLP analysis with inter-subspecific hybrid mice F1 progenies.

(C) Imprinted expression of *Rhox5/Pem* at early embryonic stages. The expression of *Rhox5/Pem* was examined in unfertilized eggs (B6) and at 2 cell, 8 cell, morula, and blastocyst stages (B6×JF1) (left panel). Allelic expression of *Rhox5/Pem* was analyzed in B6 × J F1 embryos (8 cell, morula, blastocyst, and 7.5 dpc embryonic stages; right panel).

of a family (*Rhox1-12*) whose members might compensate for loss of the *Rhox5/Pem* function. All 12 *Rhox* genes are contained within an approximately 0.7 Mb segment of the X chromosome, and expression analysis of the 12 *Rhox* genes in male and female blastocysts revealed that *Rhox9/Psx2* was also predominantly expressed in females, as with *Rhox5/Pem*. This suggests an imprinted cluster near the *Rhox5/Pem* gene.

Other X-linked imprinted genes (*Xlr3b, Xlr4b,* and *Xlr4c*) have been reported [28, 29], and their expression levels are 5–6 times higher in the developing brain of males than in females. However, *Rhox5/Pem* reported here is paternally expressed, whereas *Xlr* genes are maternally expressed. This finding of imprinted *Rhox5/Pem* indicates epigenetic differences between male and female embryos as early as the preimplantation stage. X-linked imprinted genes in general appear to affect the developmental delay of XO embryos and may be associated with later cognitive dysfunction, if they are mutated [24, 30, 31]. Thus, studies on the potential imprinted regions of *Xlr* genes and *Rhox5/Pem* may provide new insights into imprinting-related disorders.

Conclusions

Nearly 600 genes were differentially expressed between male and female blastocysts. Among these, *Xist* and *Rhox5/Pem* were expressed predominantly in females, and *Dby* and *Eif2s3y* were exclusively expressed in males. Moreover, *Rhox5/Pem* is an imprinted gene expressed from the paternally derived X chromosome, indicating epigenetic sex differences as early as the preimplantation stage.

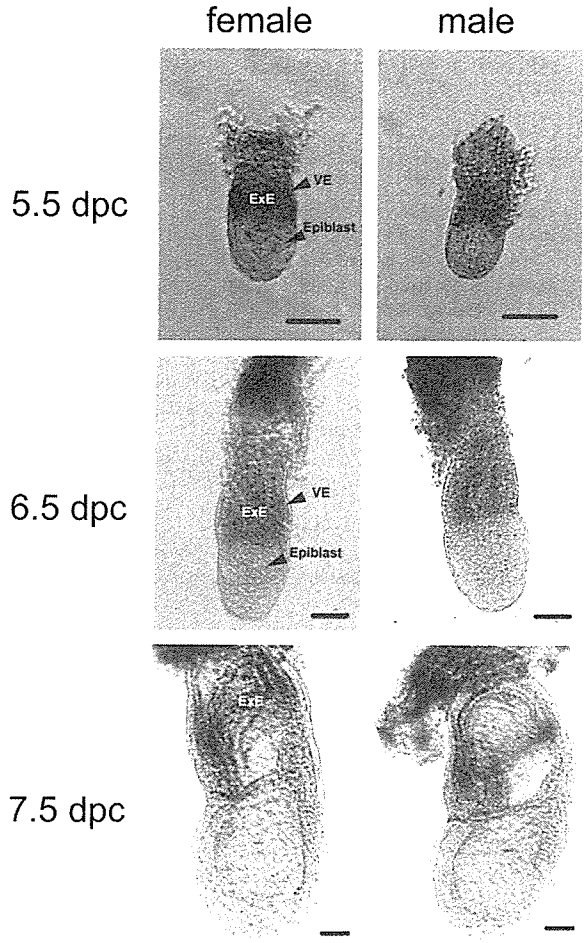

Figure 4. Expression of *Rhox5/Pem* in 5.5, 6.5, and 7.5 dpc Male and Female Embryos

No obvious differences were detected. *Rhox5/Pem* expression was detected in extraembryonic ectoderm (ExE) and visceral endoderm (VE), but not in the epiblast at 5.5 or 6.5 dpc. The expression was also detected in extraembryonic ectoderm (ExE), but not in epiblast, at 7.5 dpc. The scale bar represents 50 μm.

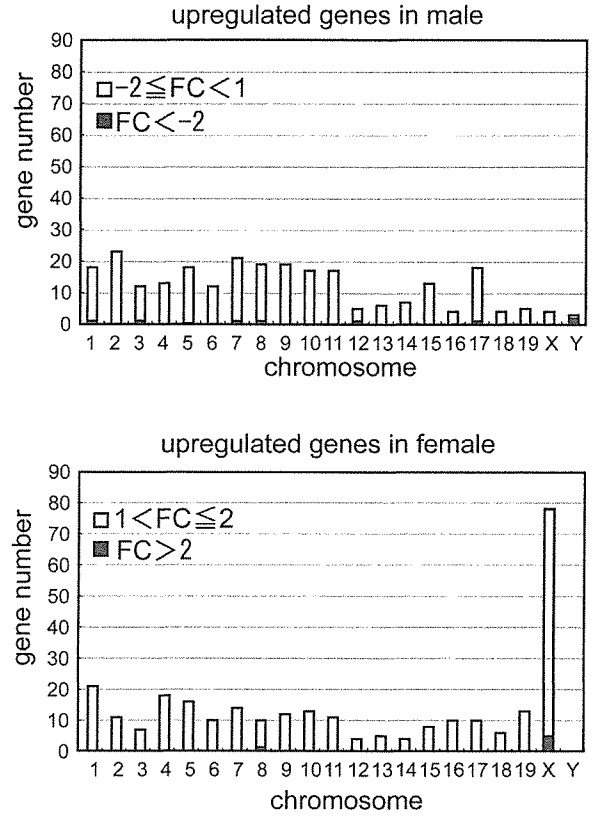

Figure 5. The Chromosomal Distribution of Differentially Expressed Genes

The upper and lower panels show upregulated genes in males and females, respectively. Open and closed bars correspond to the value of n-fold changes as shown in the figures. $p < 0.01$. The calculation methods were the same as those described in the legend for Figure 1C.

Experimental Procedures

Animals

The handling and surgical manipulation of all experimental animals were carried out according to the guidelines of the Committee on the Use of Live Animals in Teaching and Research of Osaka University. The strain B6C3F1 TgN (act EGFP) Osb CX-38 (G38) described previously [11] was used as an EGFP-expressing transgenic mouse line to distinguish between male and female embryos.

Blastocyst Collection and RNA Extraction

Eight-week-old B6C3F$_1$ female mice were superovulated with 5 IU of pregnant mare serum gonadotropin (PMSG) followed by 5 IU of human chorionic gonadotropin (hCG) 48 hr later and were mated with X^{GFP}Y male mice. Four-cell-stage embryos were collected from the oviducts 55 hr after the hCG injection, placed in kSOM, and incubated in a humidified atmosphere of 5% CO_2 in air at 37°C for an additional 38 hr. We separated male (EGFP-negative) and female (EGFP-positive) embryos at the blastocyst stage by observing green fluorescence under a dissection microscope. RNA samples were prepared from sexed blastocysts with ISOGEN (NIPPON GENE Inc., Japan), which is based on acid guanidine thiocyanate-phenol-chloroform extraction. To verify differential gene expression in non-transgenic embryos in vivo, we obtained wild-type C57BL/6 blastocysts from the uterus of superovulated C57BL/6 females mated with wild-type C57BL/6 males 92 hr after hCG injection. Genomic DNA and RNA were extracted from individual blastocysts. Male and female blastocysts were pooled separately after sex determination PCR with the following *Ube1x* primers: 5′-TGGTCTGGACCC AAACGCTGTCCACA-3′ and 5′-GGCAGCAGCCATCACATAATCCA GATG-3′ [32]. For each independent experiment, 30–40 wild-type blastocysts were sexed and pooled samples were used for expression analysis.

Comparative Expression Analysis with DNA Microarray

This is described in the GEO database of NCBI (http://www.ncbi.nlm.nih.gov/projects/geo/). The GEO accession number is GSE2934.

RT-PCR of Candidate Genes for Sexually Dimorphic Expression

Reverse transcription was carried out with the pooled total RNA extracted from 100 blastocysts via Superscript RT (Invitrogen). One hundredth of the resulting cDNA samples was amplified by PCR with *ExTaq* DNA polymerase (TaKaRa). Reaction mixtures contained 1× *ExTaq* buffer, 2.5 mM dNTP, 40 pmol of primers, and 1.25 units of *ExTaq* in a final reaction volume of 50 μl. The amplification conditions were 1 min at 96°C, followed by 30–33cycles for *Xist*, *Rhox5/Pem*, *Dby*, and *Eif2s3y* and 24 cycles for *β-actin*. Cycles were 96°C for 15 s, 65°C for 30 s, and 72°C for 30 s, with a final 1 min extension at 72°C. Primer sets were as follows: 5′-AAGTGTGACGTTGACATC CG-3′ and 5′-GATCCACATCTGCTGGAAGG-3′ for *β-actin*, 5′-CT CATCCTCATGTCTTCTCCG-3′ and 5′-GATTCCAGATAGACAGGCT GG-3′ for *Xist*, 5′-AGAGATGAGCAAGGTGCACA-3′ and 5′-CGAAC CTAGAGCCCTGGAG-3′ for *Rhox5/Pem*, 5′-CGACCATATCTTCCAT TTTCC-3′ and 5′-GCCTGGACCAGCAATTTGTTG-3′ for *Dby*, 5′-GC

CATTTCTGGTGTTCACACTG-3′ and 5′-CATAAGCTTCCCTTCTC CGTC-3′ for *Eif2s3y*. PCR primers for *Dby* and *Eif2s3y* were from [33]. All PCR reactions were repeated at least once. The same PCR conditions were used for examining the wild-type blastocysts, except the amount of starting material (30–40 blastocysts) was different.

Verification of Imprinting

Two reciprocal F_1 hybrid blastocysts, (C57BL/6 × JF1) F_1 and (JF1 × C57BL/6) F_1, were produced by an in vitro fertilization (IVF) method. In each experiment at least 30 blastocysts were sexed with a PCR-based method as described above, and blastocysts were pooled according to their sex. One third of the resulting cDNA samples derived from pooled RNAs were amplified by PCR with the above primers. To verify the imprinting status of *Rhox5/Pem*, we digested amplified PCR products with the BsrBI restriction enzyme and separated them by using an Agilent Bio Analyzer 2100 (Agilent). The allelic expression of *Rhox5/Pem* in 2 cell, 8 cell, and morula stages were analyzed with non-sexed C57BL/6 × JF1 pooled samples (20–50 pooled embryos) by RFLP analysis. Embryos (7.5 dpc) were sexed by PCR as described above; six females were pooled, and expression was analyzed. We carried out duplicate RT–PCR and RFLP analyses.

In Situ Hybridization and Histology

Mouse embryos were staged on the basis of their morphology [34]. Whole-mount in situ hybridization was performed as described in our previous paper [35]. The RNA probes encompass nucleotides 1–431 of *Rhox5/Pem* (NM_008818), and this sequence is specific to *Rhox5/Pem*.

Supplemental Data

Supplemental Data are available with this article online at http://current-biology.com/cgi/content/full/16/2/166/DC1/.

Acknowledgments

This work was supported by a Grant-in-Aid for Scientific Research from The Ministry of Education, Culture, Sports, Science, and Technology and by the 21st Century COE program from the Ministry of Education, Culture, Sports, Science, and Technology of Japan.

Received: July 13, 2005
Revised: November 7, 2005
Accepted: November 25, 2005
Published: January 23, 2006

References

1. Tsunoda, Y., Tokunaga, T., and Sugie, T. (1985). Altered sex ratio of live young after transfer of fast- and slow-developing mouse embryos. Gamete Res. *12*, 301–304.
2. Valdivia, R.P., Kunieda, T., Azuma, S., and Toyoda, Y. (1993). PCR sexing and developmental rate differences in preimplantation mouse embryos fertilized and cultured in vitro. Mol. Reprod. Dev. *35*, 121–126.
3. Jost, A. (1970). Hormonal factors in the sex differentiation of the mammalian foetus. Philos. Trans. R. Soc. Lond. B Biol. Sci. *259*, 119–130.
4. Hartshorn, C., Rice, J.E., and Wangh, L.J. (2002). Developmentally-regulated changes of *Xist* RNA levels in single preimplantation mouse embryos, as revealed by quantitative real-time PCR. Mol. Reprod. Dev. *61*, 425–436.
5. Kay, G.F., Barton, S.C., Surani, M.A., and Rastan, S. (1994). Imprinting and X chromosome counting mechanisms determine *Xist* expression in early mouse development. Cell *77*, 639–650.
6. Gutierrez-Adan, A., Oter, M., Martinez-Madrid, B., Pintado, B., and De La Fuente, J. (2000). Differential expression of two genes located on the X chromosome between male and female in vitro-produced bovine embryos at the blastocyst stage. Mol. Reprod. Dev. *55*, 146–151.
7. Peippo, J., Farazmand, A., Kurkilahti, M., Markkula, M., Basrur, P.K., and King, W.A. (2002). Sex-chromosome linked gene expression in in-vitro produced bovine embryos. Mol. Hum. Reprod. *8*, 923–929.
8. Larson, M.A., and Kubisch, H.M. (1999). The effects of group size on development and interferon-tau secretion by in-vitro fertilized and cultured bovine blastocysts. Hum. Reprod. *14*, 2075–2079.
9. Zwingman, T., Erickson, R.P., Boyer, T., and Ao, A. (1993). Transcription of the sex-determining region genes *Sry* and *Zfy* in the mouse preimplantation embryo. Proc. Natl. Acad. Sci. USA *90*, 814–817.
10. Hadjantonakis, A.K., Gertsenstein, M., Ikawa, M., Okabe, M., and Nagy, A. (1998). Non-invasive sexing of preimplantation stage mammalian embryos. Nat. Genet. *19*, 220–222.
11. Nakanishi, T., Kuroiwa, A., Yamada, S., Isotani, A., Yamashita, A., Tairaka, A., Hayashi, T., Takagi, T., Ikawa, M., Matsuda, Y., et al. (2002). FISH analysis of 142 EGFP transgene integration sites into the mouse genome. Genomics *80*, 564–574.
12. Okabe, M., Ikawa, M., Kominami, K., Nakanishi, T., and Nishimune, Y. (1997). 'Green mice' as a source of ubiquitous green cells. FEBS Lett. *407*, 313–319.
13. Huynh, K.D., and Lee, J.T. (2003). Inheritance of a pre-inactivated paternal X chromosome in early mouse embryos. Nature *426*, 857–862.
14. Mak, W., Nesterova, T.B., de Napoles, M., Appanah, R., Yamanaka, S., Otte, A.P., and Brockdorff, N. (2004). Reactivation of the paternal X chromosome in early mouse embryos. Science *303*, 666–669.
15. Okamoto, I., Otte, A.P., Allis, C.D., Reinberg, D., and Heard, E. (2004). Epigenetic dynamics of imprinted X inactivation during early mouse development. Science *303*, 644–649.
16. Avery, B., Jorgensen, C.B., Madison, V., and Greve, T. (1992). Morphological development and sex of bovine in vitro-fertilized embryos. Mol. Reprod. Dev. *32*, 265–270.
17. Yadav, B.R., King, W.A., and Betteridge, K.J. (1993). Relationships between the completion of first cleavage and the chromosomal complement, sex, and developmental rates of bovine embryos generated in vitro. Mol. Reprod. Dev. *36*, 434–439.
18. Pergament, E., Fiddler, M., Cho, N., Johnson, D., and Holmgren, W.J. (1994). Sexual differentiation and preimplantation cell growth. Hum. Reprod. *9*, 1730–1732.
19. Bernardi, M.L., and Delouis, C. (1996). Sex-related differences in the developmental rate of in-vitro matured/in-vitro fertilized ovine embryos. Hum. Reprod. *11*, 621–626.
20. Cassar, G., King, W.A., and King, G.J. (1994). Influence of sex on early growth of pig conceptuses. J. Reprod. Fertil. *101*, 317–320.
21. Banzai, M., Omoe, K., Ishikawa, H., and Endo, A. (1995). Viability, development and incidence of chromosome anomalies of preimplantation embryos from XO mice. Cytogenet. Cell Genet. *70*, 273–277.
22. Burgoyne, P.S. (1993). A Y-chromosomal effect on blastocyst cell number in mice. Development *117*, 341–345.
23. Burgoyne, P.S., Thornhill, A.R., Boudrean, S.K., Darling, S.M., Bishop, C.E., and Evans, E.P. (1995). The genetic basis of XX–XY differences present before gonadal sex differentiation in the mouse. Philos. Trans. R. Soc. Lond. B Biol. Sci. *350*, 253–260.
24. Thornhill, A.R., and Burgoyne, P.S. (1993). A paternally imprinted X chromosome retards the development of the early mouse embryo. Development *118*, 171–174.
25. Maclean, J.A., 2nd, Chen, M.A., Wayne, C.M., Bruce, S.R., Rao, M., Meistrich, M.L., Macleod, C., and Wilkinson, M.F. (2005). Rhox: A new homeobox gene cluster. Cell *120*, 369–382.
26. Arnaud, P., Monk, D., Hitchins, M., Gordon, E., Dean, W., Beechey, C.V., Peters, J., Craigen, W., Preece, M., Stanier, P., et al. (2003). Conserved methylation imprints in the human and mouse *GRB10* genes with divergent allelic expression suggests differential reading of the same mark. Hum. Mol. Genet. *12*, 1005–1019.
27. Hikichi, T., Kohda, T., Kaneko-Ishino, T., and Ishino, F. (2003). Imprinting regulation of the murine *Meg1/Grb10* and human *GRB10* genes; roles of brain-specific promoters and mouse-specific CTCF-binding sites. Nucleic Acids Res. *31*, 1398–1406.
28. Davies, W., Isles, A., Smith, R., Karunadasa, D., Burrmann, D., Humby, T., Ojarikre, O., Biggin, C., Skuse, D., Burgoyne, P., et al. (2005). *Xlr3b* is a new imprinted candidate for X-linked

parent-of-origin effects on cognitive function in mice. Nat. Genet. *37*, 625–629.
29. Raefski, A.S., and O'Neill, M.J. (2005). Identification of a cluster of X-linked imprinted genes in mice. Nat. Genet. *37*, 620–624.
30. Jamieson, R.V., Tan, S.S., and Tam, P.P. (1998). Retarded post-implantation development of X0 mouse embryos: Impact of the parental origin of the monosomic X chromosome. Dev. Biol. *201*, 13–25.
31. Skuse, D.H., James, R.S., Bishop, D.V., Coppin, B., Dalton, P., Aamodt-Leeper, G., Bacarese-Hamilton, M., Creswell, C., McGurk, R., and Jacobs, P.A. (1997). Evidence from Turner's syndrome of an imprinted X-linked locus affecting cognitive function. Nature *387*, 705–708.
32. Chuma, S., and Nakatsuji, N. (2001). Autonomous transition into meiosis of mouse fetal germ cells in vitro and its inhibition by gp130-mediated signaling. Dev. Biol. *229*, 468–479.
33. Dewing, P., Shi, T., Horvath, S., and Vilain, E. (2003). Sexually dimorphic gene expression in mouse brain precedes gonadal differentiation. Brain Res. Mol. Brain Res. *118*, 82–90.
34. Downs, K.M., and Davies, T. (1993). Staging of gastrulating mouse embryos by morphological landmarks in the dissecting microscope. Development *118*, 1255–1266.
35. Yamamoto, M., Saijoh, Y., Perea-Gomez, A., Shawlot, W., Behringer, R.R., Ang, S.L., Hamada, H., and Meno, C. (2004). Nodal antagonists regulate formation of the anteroposterior axis of the mouse embryo. Nature *428*, 387–392.

BIOLOGY OF REPRODUCTION 75, 760–766 (2006)
Published online before print 26 July 2006.
DOI 10.1095/biolreprod.106.052977

Aberrant Distribution of ADAM3 in Sperm from Both Angiotensin-Converting Enzyme (*Ace*)- and Calmegin (*Clgn*)-Deficient Mice[1]

Ryo Yamaguchi,[3,6,7] Kazuo Yamagata,[3,4,6] Masahito Ikawa,[8] Stuart B. Moss,[5,6] and Masaru Okabe[2,6,7]

Genome Information Research Center,[6] Pharmaceutical Sciences,[7] Research Institute for Microbial Diseases,[8] Osaka University, Osaka, 565-0871, Japan

ABSTRACT

Male mice deficient for the calmegin (*Clgn*) or the angiotensin-converting enzyme (*Ace*) gene show impaired sperm migration into the oviduct and loss of sperm-zona pellucida binding ability in vitro. Since CLGN is a molecular chaperone for membrane transport of target proteins and ACE is a membrane protein, we looked for ACE on the sperm membranes from *Clgn*$^{-/-}$ mice. ACE was present and showed normal activity, indicating that CLGN is not involved in transporting ACE to the sperm membranes. The ablation of the *Adam2* and *Adam3* genes generated animals whose sperm did not bind the zona pellucida, which led us to examine the presence of ADAM2 and ADAM3 in *Clgn*$^{-/-}$ and *Ace*$^{-/-}$ sperm. ADAM3 was absent from *Clgn*$^{-/-}$ sperm. In the *Ace*$^{-/-}$ mice, while ADAM2 was found normally in the sperm, ADAM3 disappeared from the Triton X-114 detergent-enriched phase after phase separation, which suggests that ACE is involved in distributing ADAM3 to a location where it can participate in sperm-zona pellucida binding. This diminished amount of ADAM3 in the Triton X-114 detergent-enriched phase may explain the inability of *Clgn*$^{-/-}$ and *Ace*$^{-/-}$ sperm to bind to the zona pellucida.

gamete biology, in vitro fertilization, male sexual function, sperm capacitation

INTRODUCTION

Mammalian fertilization is accomplished through complex processes that involve cell–matrix and cell–cell interactions. The zona pellucida (ZP) is an extracellular matrix that serves as a barrier to protect the egg from physiological damage [1] and to block polyspermic fertilization. Based on biochemical analyses, different sperm proteins have been postulated to play roles in ZP binding, penetration and fusion. However, when genes, such as *Acr* (acrosin) [2], *B4galt1* [3], *Spam1* (previously known as PH-20) [4], *Mfge8* (previously known as SED1) [5], and *Cd46* [6] are ablated, the predicted phenotypes do not appear, which suggests that the various models used to explain fertilization need to be redefined. Among the various proteins that have been reported to have critical roles in fertilization, only the A Disintegrin And Metalloprotease 2 (*Adam2*) gene (previously known as fertilin-β) has been shown to be essential [7]. Even in this case, the observed phenotype, i.e., loss of ZP-binding ability, is different from that of the predicted phenotype, i.e., a role in sperm-egg fusion. Additional proteins that may play roles in sperm-ZP binding have emerged over the years. For example, we have shown that the calmegin (*Clgn*) gene is essential for sperm binding to the ZP [8]. Other genes, such as *Adam1a and Adam3*, as well as the angiotensin-converting enzyme *(Ace)*, have also emerged as essential factors for sperm-ZP binding [9–11].

It is intriguing that the disruption of certain genes, e.g., *Clgn*, *Ace*, *Adam1a*, *Adam2*, and *Adam3*, results in a similar sperm phenotype, i.e., failure of sperm to bind to the ZP. Since CLGN functions as a testis-specific molecular chaperone, we previously examined the possibility of ADAM2 misfolding in sperm from *Clgn*$^{-/-}$ mice [12]. In wild-type sperm, both ADAM1 and ADAM2 bind CLGN and this interaction probably leads to the correct tertiary folding of these proteins. However, in the absence of CLGN, the ADAM1/ADAM2 heterodimer disappears from testicular extracts. Subsequently, it has been shown that the *Adam1* gene comprises two similar genes, *Adam1a* and *Adam1b*, and that only ADAM1b is present in sperm, where it forms a heterodimer with ADAM2 [13, 14]. It is clear that when the ADAM1b/ADAM2 heterodimer fails to assemble in the testis, ADAM2 disappears from the sperm of the *Clgn*$^{-/-}$ male mouse. These results helped to clarify why *Clgn*$^{-/-}$ and *Adam2*$^{-/-}$ mice share a similar phenotype, i.e., the sperm cannot bind to the ZP because they lack ADAM2.

To continue our studies towards deciphering the role of candidate genes in sperm-ZP binding, we turned our attention to the angiotensin-converting enzyme. Somatic ACE (sACE) is a zinc metalloprotease that is involved in blood pressure regulation by cleaving bioactive peptides, such as angiotensin I and bradykinin. Testicular ACE (tACE) has also been described, and is generated by alternative promoter usage [15]. Both isoforms have similar enzymatic activities. Ablation of both sACE and tACE results in males with reduced fertility [16]. Males that lack only sACE are fertile, which indicates that tACE is responsible for the infertility [17, 18]. We now report a role of tACE in the localization of ADAM3 so that it can participate in sperm-zona pellucida binding.

MATERIALS AND METHODS

Animals

Clgn$^{+/-}$ and *Clgn*$^{-/-}$ male mice were obtained by mating *Clgn*$^{-/-}$ females with *Clgn*$^{+/-}$ males. The *Ace*$^{-/-}$ mice were originally produced by Krege et al. [9]. Mice heterozygous for alterations in exon 14 of the *Ace* gene, which contains critical amino acids for sACE and tACE functions [15], were purchased from the Jackson Laboratory (Bar Harbor, ME). *Ace*$^{+/-}$ and *Ace*$^{-/-}$

[1]Supported by grants (11234203 and 00531), a grant-in-aid for Scientific Research, and the 21st Century 200 COE program from the Ministry of Education, Culture, Sports, Science, and Technology of Japan, and by NIH HD06274 (S.B.M.).
[2]Correspondence: Masaru Okabe, Genome Information Research Center, Osaka University, Yamadaoka 3–1, Suita, Osaka, 565-0871, Japan. FAX: 81 6 6879 8376; e-mail: okabe@gen-info.osaka-u.ac.jp
[3]These authors contributed equally to this work.
[4]Current address: Graduate School of Life and Environmental Sciences, Tsukuba University, Tsukuba Science City, Ibaraki 305-8572, Japan.
[5]On sabbatical leave from the Center for Research on Reproduction and Women's Health, University of Pennsylvania Medical Center, Philadelphia, PA 19104.

Received: 4 April 2006.
First decision: 26 April 2006.
Accepted: 17 July 2006.

ISSN: 0006-3363. http://www.biolreprod.org

male mice were obtained by mating $Ace^{+/-}$ females with $Ace^{+/-}$ males. All of the experiments were performed with the approval of the Animal Care and Use Committee of Osaka University.

Antibodies

Affinity-purified rabbit anti-ADAM1a (1aCysE), anti-ADAM1b (1bCysE), and anti-SPAM1 (previously known as PH-20) [4, 13] antibodies, which were produced by immunizing with recombinant proteins that correspond to a unique region within each protein, were kind gifts from Drs. Hitoshi Nishimura and Tadashi Baba (University of Tsukuba, Ibaraki, Japan). Monoclonal antibodies (Mabs) against mouse ADAM2 (fertilin-β; 9D2.2) and ADAM3 (cyritestin; 7C1.2) were purchased from Chemicon International Inc. (Temecula, CA). Rabbit anti-SPAM1 antiserum [19] was a kind gift from Dr. Paul Primakoff (University of California, Davis, CA). Affinity-purified antibodies against ADAM2, IZUMO1, CD46, and CLGN were obtained as described previously [6, 8, 12, 20]. The rat anti-mouse sperm tail antigen Mab (#124) was generated in our laboratory and was used to examine the separation of sperm heads and tails.

To produce monoclonal antibodies against ACE, we prepared an amino-terminal recombinant tACE protein (AA #31–140). A DNA fragment that contained 110 amino acids starting from the N-terminus of the mature form of tACE (without the signal peptide) was obtained by PCR-amplification using a forward primer that corresponds to nucleotides 89–113 (5′-TTCCATGGC-CACTGACCACGTGACAGCCAA-3′) and a reverse primer that corresponds to nucleotides 399–420 (5′-ACTCGAGAGAGTTTTGAAAGTTGCTCAC-3′). The DNA was ligated into the *Nco*I and *Xho*I restriction sites of pET28b (Novagen, Madison, WI) and transformed. The recombinant tACE protein was expressed as a fusion protein with the 6×His tag at the C-terminus, and purified by Ni-NTA resin affinity column chromatography (Qiagen, Hilden, Germany). Monoclonal antibodies against ACE were generated by MBL (Nagoya, Japan). Two 7-week-old, female $Ace^{-/-}$ mice were immunized i.p. with 50 μg of recombinant protein emulsified in complete Freunds adjuvant (Day 0) or incomplete Freunds adjuvant (Days 7, 14, 21, and 28). Spleen cells were harvested three days after the fifth immunization and fused with mouse myeloma cells using polyethylene glycol. Wells that contained hybridomas were screened by an enzyme-linked immunosorbent assay (ELISA) for recombinant tACE protein. Positive clones were grown, and their supernatants were used for further screening. The supernatant from one clone, 1D5, was used for immunoblot analysis.

Fractionation of Sperm Heads and Tails

Sperm from the cauda epididymis and vas deferens were collected in TBS. Sperm heads and tails were separated by mild sonication on ice (five times with flash set at output level 1) using the Ultrasonic Disruptor UD-201 (Tomy Digital Biology, Tokyo, Japan), followed by the addition of an equal amount of 1.8 M sucrose. The 2-ml sample was layered on a discontinuous sucrose gradient composed of 2 ml of 0.9 M sucrose, 1 ml of 2.05 M sucrose, and 1 ml of 2.2 M sucrose; all of the sucrose solutions contained 10 mM Tris-HCl (pH 7.5) and 0.15 M NaCl. The gradients were centrifuged at 100 000 × *g* for 12 h in a SW50.1 rotor (Beckman Coulter, Tokyo, Japan). Sperm tails banded at the 0.9 M/2.05 M interface, and the sperm heads were found in the pellet. Both fractions were resuspended in TBS and pelleted by centrifugation at 1000 × *g* for 10 min. The samples were subjected to immunoblot analysis, as described below.

Phase Separation of Sperm Triton X-114 Extracts

Cauda epididymal and vas deferens sperm were collected into PBS and centrifuged at 1000 × *g* for 10 min at 4°C. The sperm pellets were suspended in PBS that contained 1% Triton X-114 [21], 10 mM benzamidine, 0.5 mM PMSF, 1 μg/ml leupeptin, and 1 μg/ml pepstatin A. The sperm suspensions were placed on ice for 20 min with occasional vortexing. After centrifuging at 15 700 × *g* for 20 min at 4°C, the supernatants were collected, and layered onto 6% sucrose/PBS in microtubes. After incubation at 37°C for 15 min, the tubes were centrifuged at 1000 × *g* for 15 min at room temperature, to separate the Triton X-114 extract into the detergent-depleted phase, sucrose phase, and detergent-enriched phase. The separated detergent-depleted and detergent-enriched phases were mixed with SDS-sample buffer, boiled, and subjected to SDS-PAGE and immunoblot analysis.

Immunoblot Analysis

Sperm from the cauda epididymis and vas deferens of sexually mature male mice were collected and incubated in lysis buffer (10 mM Tris-HCl [pH 7.5], 50 mM KCl, 1% Triton X-100, 10 mM benzamidine, 0.5 mM PMSF, 1 μg/ml leupeptin, 1 μg/ml pepstatin A) for 20 min on ice with occasional vortexing. The testis and kidney were excised, minced, and homogenized in lysis buffer, and then placed on ice for 1 h. The sperm and tissue extracts were pelleted at 15 700 × *g* for 5 min at 4°C, and the supernatants were collected. The protein concentration in each homogenate was determined using the Coomassie protein assay reagent (Pierce, Rockford, IL). Proteins were separated by SDS-PAGE under reducing conditions (CLGN, ADAM2, ADAM3, ACE, SPAM1, and #124) or non-reducing conditions (ADAM1b, IZUMO1, and CD46), and were transferred electrophoretically to PVDF membranes (Immobilon-P; Millipore Corp., Bedford, MA). After blocking in TBS-T buffer (20 mM Tris-HCl [pH 7.5], 150 mM NaCl, 0.05% Tween-20] that contained 5% skim milk, the blots were incubated with primary antibody overnight at 4°C, and then incubated with horseradish peroxidase-conjugated goat anti-rabbit IgG or goat anti-mouse IgG (GE Healthcare Bio-Sciences Corp., Piscataway, NJ). The detection of immunoreactive bands was performed using the enhanced chemiluminescence (ECL) Western blotting detection kit (GE Healthcare Bio-Sciences). Signal intensities were determined using the Scion Image software (Scion Corp., Frederick, MD).

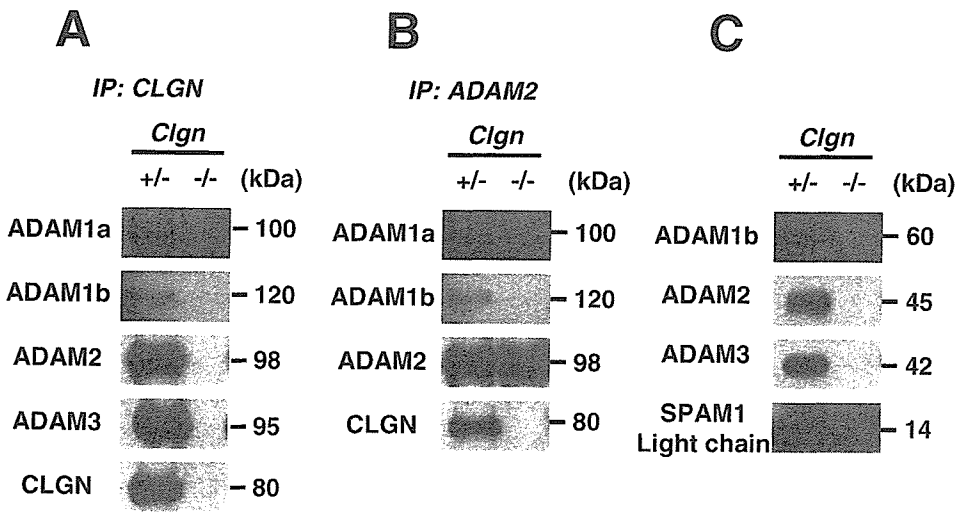

FIG. 1. The presence of ADAMs in the testes and sperm of $Clgn^{-/-}$ mice. Proteins from $Clgn^{+/-}$ and $Clgn^{-/-}$ testis and sperm were subjected to immunoprecipitation and immunoblot analysis. **A**) Association of ADAMs with CLGN. Testicular proteins from animals of each genotype were immunoprecipitated with the anti-CLGN antibody. The precipitates were subjected to immunoblot analysis using antibodies against ADAM1a, ADAM1b, ADAM2, ADAM3, and CLGN. **B**) Heterodimerization of ADAM2/1a and ADAM2/1b. Testicular proteins from animals of each genotype were immunoprecipitated using the anti-ADAM2 antibody, followed by immunoblot analysis using antibodies to ADAM1a, ADAM1b, and ADAM2. **C**) Detection of ADAMs in sperm. Sperm proteins from animals of each genotype were separated by electrophoresis and subjected to immunoblot analysis using antibodies to ADAM1b, ADAM2, and ADAM3. As a control, the light chain of SPAM1 is detected with anti-SPAM1 antiserum in both the $Clgn^{+/-}$ and $Clgn^{-/-}$ sperm.

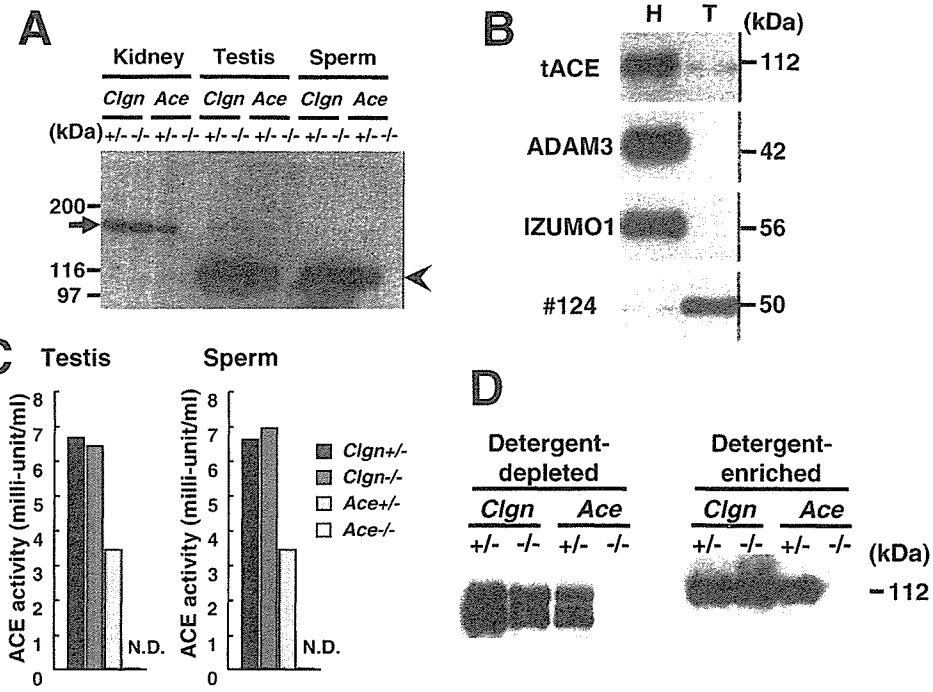

FIG. 2. The presence of ACE in the testes and sperm of *Clgn*$^{-/-}$ mice. **A**) The anti-ACE antibody recognized both somatic and testicular ACE. Kidney (100 μg), testis (50 μg), and sperm (20 μg) proteins from *Clgn* and *Ace*$^{+/-}$ and *Ace*$^{-/-}$ animals were separated by electrophoresis and subjected to immunoblot analysis using the anti-ACE monoclonal antibody (1D5). Somatic ACE (arrow) and testicular ACE (arrowhead) are denoted. **B**) ACE is present in the sperm head. Sperm heads (H) and tails (T) were prepared and subjected to immunoblot analysis using antibodies to ACE, ADAM3, IZUMO1, and a tail-specific antigen (#124). **C**) ACE activities in testis and sperm homogenates from *Clgn* and *Ace*$^{+/-}$ and *Ace*$^{-/-}$ animals. N.D., not detected. **D**) Testicular ACE is present in the detergent-enriched phase of the sperm. Sperm proteins were partitioned into detergent-depleted and detergent-enriched phases by extraction with 1% Triton X-114, and subjected to immunoblot analysis using the anti-ACE antibody.

Immunoprecipitation

Testes were collected and homogenized in lysis buffer using the Potter-Elvehjem homogenizer with 10 strokes at 1000 rpm. The homogenates were placed on ice for 1 h with occasionally vortexing, and then centrifuged at 15 700 × *g* for 5 min at 4°C. The supernatants were collected and precleared by the addition of protein A-Sepharose (GE Healthcare Bio-Sciences) overnight at 4°C. After centrifugation, antibodies were added to the supernatants, and the solutions were incubated with rocking for 3 h at 4°C. Protein A–Sepharose was then added to each tube, and incubation was allowed to continue for 2 h at 4°C. After washing four times with lysis buffer, the final pellet was resuspended in 8 M urea and SDS–PAGE loading buffer, boiled for 3 min, and the proteins were separated by SDS–PAGE under reducing conditions.

Measurement of ACE Activity

Testis and sperm homogenates were prepared as described above. The protein concentration of each homogenate was adjusted to 0.2 mg/ml with lysis buffer, and 100 μl of each sample was applied to a MicroSpinTM G-25 column (GE Healthcare Bio-Sciences), to remove residual salt. The activity of ACE in each homogenate was measured using the Angiotensin-I Converting Enzyme Activity Assay Kit (Yagai Research Center, Yamagata, Japan) according to the manufacturers protocol.

Sperm-ZP Binding Assay

The in vitro assays for sperm binding to zona pellucida were performed with eggs from which the cumulus cells had been removed by treatment with bovine testicular hyaluronidase (175 U/ml; Sigma) for 5 min. In brief, cumulus-free eggs from female B6D2F1 mice (>2 months old; Japan SLC, Inc., Shizuoka, Japan) were placed in a 200-μl drop of modified Krebs-Ringer bicarbonate solution (TYH medium) that contained glucose, sodium pyruvate, bovine serum albumin, and antibiotics [22]. An aliquot of capacitated sperm (2 × 10^5 sperm/ml) from *Clgn*$^{-/-}$ or *Ace*$^{-/-}$ males and their wild-type littermates was inseminated and the mixture were incubated for 30 min at 37°C under 5% CO_2 in air. Eggs were fixed and the bound sperm were observed with an IX-70 fluorescent microscope (Olympus) after Hoechst 33258 staining.

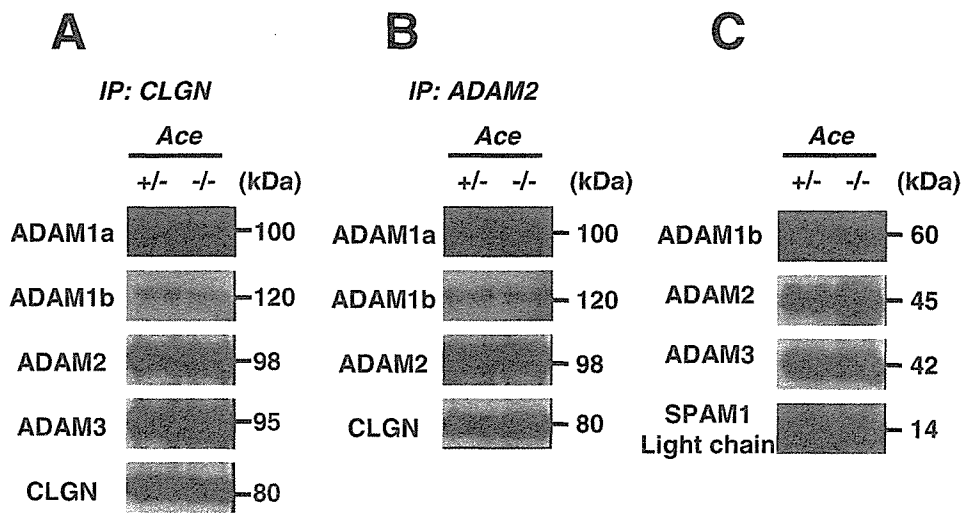

FIG. 3. The presence of ADAMs in the testes and sperm of *Ace*$^{-/-}$ mice. Proteins from *Ace*$^{+/-}$ and *Ace*$^{-/-}$ testes and sperm were subjected to immunoprecipitation and immunoblot analysis. **A**) Association of CLGN with ADAMs. Testicular proteins from animals of each genotype were immunoprecipitated with the anti-CLGN antibody. The precipitants were subjected to immunoblot analysis using antibodies to ADAM1a, ADAM1b, ADAM2, ADAM3, and CLGN. **B**) Heterodimerization of ADAM2/1a and ADAM2/1b. Testicular proteins from animals of each genotype were immunoprecipitated by the anti-ADAM2 polyclonal antibody, followed by immunoblot analysis using antibodies to ADAM1a, ADAM1b, and ADAM2. **C**) Detection of ADAMs in sperm. Sperm proteins from animals of each genotype were separated by electrophoresis and subjected to immunoblot analysis using antibodies to ADAM1b, ADAM2, and ADAM3. As a control, the light chain of SPAM1 is detected with anti-SPAM1 antiserum in both the *Ace*$^{+/-}$ and *Ace*$^{-/-}$ sperm.

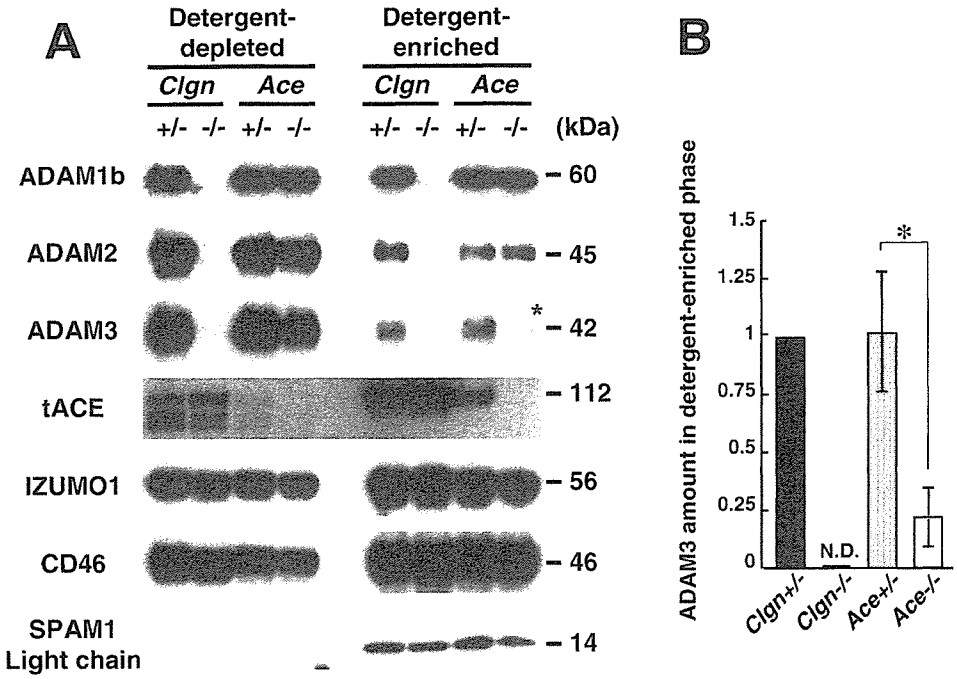

FIG. 4. ADAM3 is not localized correctly in $Ace^{-/-}$ sperm. **A**) Sperm proteins from *Clgn* and $Ace^{+/-}$ and $Ace^{-/-}$ animals were extracted with 1% Triton X-114. The detergent-depleted and detergent-enriched phases were separated by electrophoresis and subjected to immunoblot analysis using antibodies to ADAM1b, ADAM2, ADAM3, ACE, IZUMO1, CD46, and SPAM1. **B**) The amounts of sperm ADAM3 in the detergent-enriched fractions of these mice were estimated using the Scion Image software. The intensities of the signals were measured and normalized to the $Clgn^{+/-}$ value. Error bars represent mean ± SD from five independent experiments. *$P < 0.01$ (Student *t*-test).

RESULTS

ADAMs Are Present in Clgn-Deficient Mouse Testes But Not in Sperm

Since disruption of the genes that encode *Adam1a*, *Adam2*, and *Adam3* results in a male sterility phenotype that is similar to that seen for $Clgn^{-/-}$ animals [7, 8, 10, 11], we analyzed whether these ADAMs are present in the testis and sperm of CLGN-null mice. When a testicular extract from $Clgn^{+/-}$ mice was immunoprecipitated with anti-CLGN antibody and the resulting precipitate was subjected to immunoblot analysis using antibodies to ADAM1a, ADAM1b, ADAM2, and ADAM3, all of the ADAMs were detected (Fig. 1A). These results indicate that CLGN interacts with ADAMs in the testis.

As expected, the ADAMs in the testes of $Clgn^{-/-}$ mice were not immunoprecipitated by the anti-CLGN antibody. Even though the ADAMs were present in $Clgn^{-/-}$ males (data not shown), the ADAM1a/ADAM2 and ADAM1b/ADAM2 heterodimers were absent after the testicular extract was immunoprecipitated with the anti-ADAM2 antibody and the precipitate was probed with the various ADAM antibodies, which indicates that CLGN is involved in the formation of these heterodimers (Fig. 1B). In contrast, these heterodimers were observed in the $Clgn^{+/-}$ mice. We also examined the effect of CLGN disruption on ADAM3, as it has been previously reported that the absence of the ADAM1a/ADAM2 heterodimer due to ADAM1a disruption leads to the disappearance of sperm ADAM3 [10, 23]. ADAM3, as well as

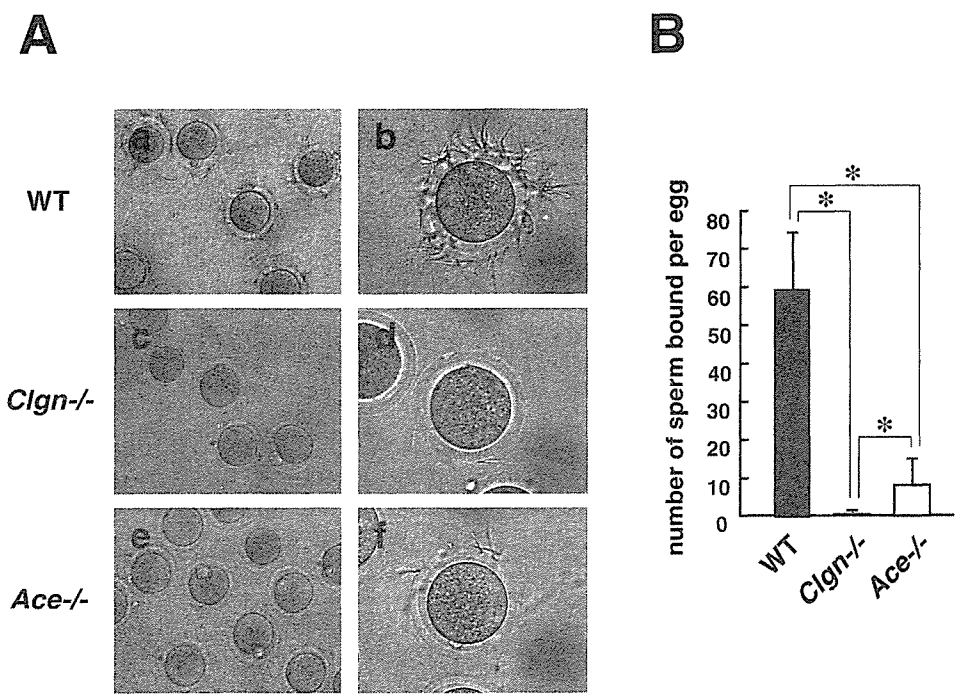

FIG. 5. Sperm from $Clgn^{-/-}$ and $Ace^{-/-}$ mice do not bind to the zona pellucida. **A**) Sperm from wild-type (**a** and **b**), $Clgn^{-/-}$ (**c** and **d**) or $Ace^{-/-}$ (**e** and **f**) mice were capacitated for 1 h and incubated with cumulus-free eggs. After 1 h, the eggs were fixed and the sperm bound to the zona pellucida were counted. Original magnification 200 (**a**, **c**, **e**) and ×400 (**b**, **d**, **f**). **B**) Error bars indicate the means ± SD from three independent experiments. *$P < 0.001$ (Student *t*-test).

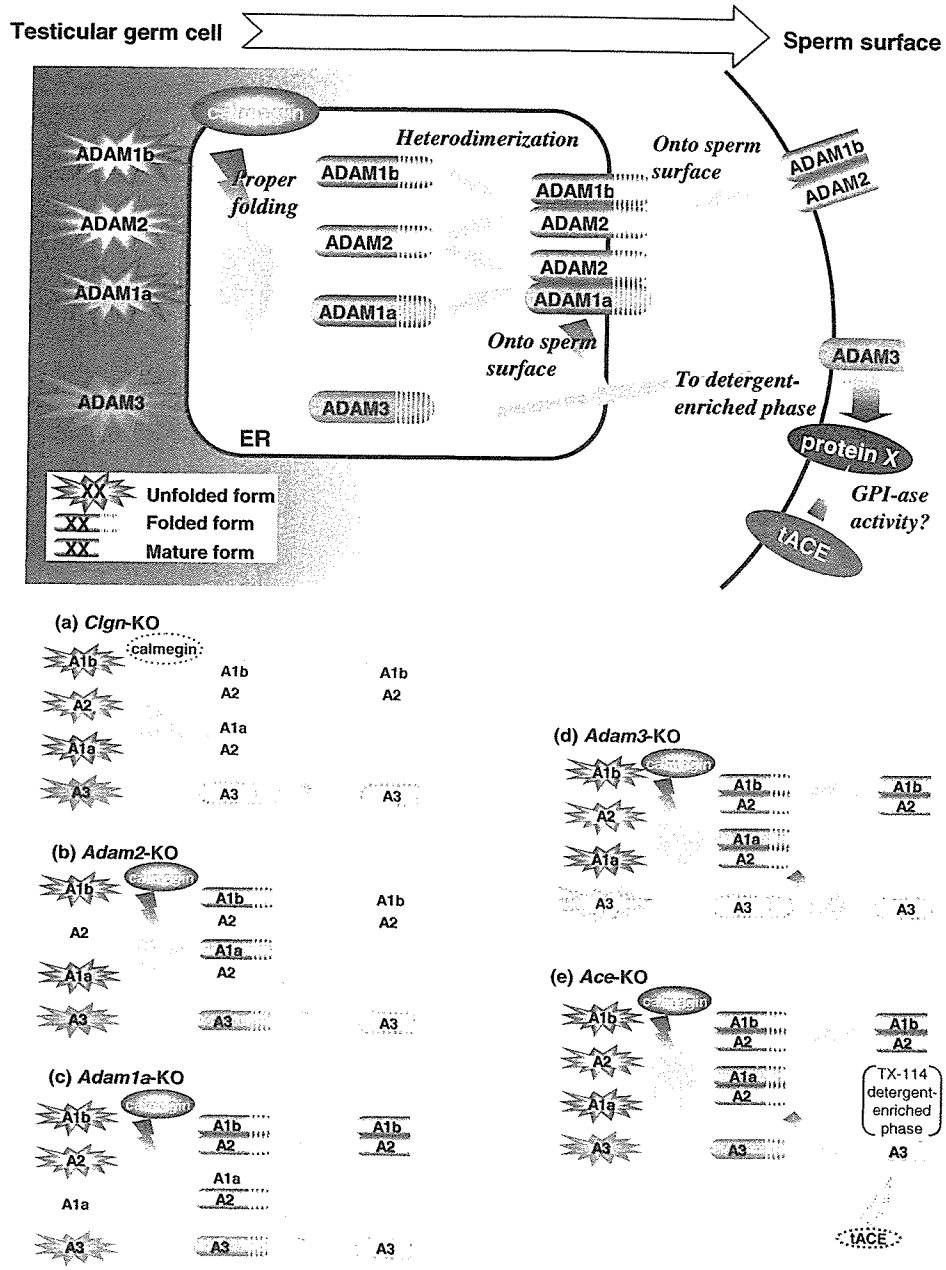

FIG. 6. Schematic model for ADAMs and their roles in sperm function. The disruption of the genes that encode *Adam1a*, *Adam2*, and *Adam3* results in impaired sperm-ZP binding. CLGN is required for the folding of ADAM1a, ADAM1b, and ADAM2 and the subsequent dimerization of these proteins. The ADAM1a/ADAM2 heterodimer is reported to be necessary for localizing ADAM3 to the sperm surface [10]. In $Clgn^{-/-}$ (**a**) and $Adam2^{-/-}$ (**b**) sperm, the disappearance of the ADAM1a/ADAM2 and ADAM1b/ADAM2 heterodimers results in the loss of ADAM1b, ADAM2, and ADAM3 from the sperm. ADAM1a is a testis-specific protein that is not found in sperm [13]. When ADAM1a is eliminated (**c**), the ADAM1a/ADAM2 heterodimer disappears from the testis, whereas the expression of ADAM1b/ADAM2 is not affected. However, these sperm lack ADAM3 [10]. The disruption of ADAM3 (**d**) is reported to have no significant effect on ADAM1a, ADAM1b or ADAM2 [27]. These findings suggest that ADAM3 is located downstream of these other ADAM proteins. In the present paper, we show that the disruption of tACE leads to the aberrant localization of ADAM3 (**e**), most likely due to a different pathway from the one hypothesized for CLGN/ADAMs. These results indicate the importance of ADAM3 in sperm-ZP interaction and explain why disruption of the individual *Ace*, *Clgn*, *Adam1a*, *Adam2*, and *Adam3* genes produces similar phenotypes.

ADAM1b and ADAM2, were not present in $Clgn^{-/-}$ sperm, which suggests that infertility is due to the disappearance of the ADAMs in this sperm population (Fig. 1C).

ACE Is Present and Localizes Normally in $Clgn^{-/-}$ Sperm

Since the sperm from $Clgn^{-/-}$ and $Ace^{-/-}$ mice show impaired migration into the oviduct and ZP-binding ability, we tested whether CLGN controls tertiary folding of the ACE protein, as it does for the ADAMs. To generate antibodies specific for ACE, we immunized $Ace^{-/-}$ female mice with the recombinant N-terminal region of the mouse tACE protein. All of the monoclonal antibodies obtained recognized both sACE and tACE and worked well for immunoblotting (but not for immunostaining). Immunoblot analysis of kidney proteins with the anti-ACE antibody detected a band with M_r ~158 000, which is consistent with the molecular mass of sACE (Fig. 2A). In testicular and sperm extracts, a band with M_r ~112 000 was detected, which is similar to the size calculated for tACE. Both bands disappeared in $Ace^{-/-}$ mice, which indicates that these bands are sACE and tACE, respectively.

After fractionation of the sperm heads and tails, tACE was found only in the head fraction from wild-type sperm (Fig. 2B). As expected, ADAM3 and IZUMO1 were also found exclusively in sperm heads, while an antigen that was recognized by the anti-sperm tail-specific Mab (#124) was found only in the tails. The $Clgn^{-/-}$ sperm had normal levels of tACE, which indicates that the lack of CLGN has no effect on the appearance of tACE (Fig. 2A). This result is supported by the finding that ACE was not immunoprecipitated from the $Clgn^{+/-}$ testicular extract by the anti-CLGN antibody (data not shown). When tACE peptidase activity was measured, tACE was found to be biologically active in $Clgn^{-/-}$ testis and sperm at levels comparable to those seen in $Clgn^{+/-}$ mice (Fig. 2C). After phase separation of sperm with Triton X-114, the band

with M_r ~112 000 was detected only in the detergent-enriched phases of the $Ace^{+/-}$ and $Clgn^{+/-}$ sperm (Fig. 2D). The smaller bands in the detergent-depleted phase most likely reflect processed and solubilized forms of tACE. A similar fractionation pattern was found for the tACE of $Clgn^{-/-}$ sperm, which suggests that tACE is not directly involved in sperm-ZP interactions.

ADAMs are Present in the $Ace^{-/-}$ Testis and Sperm

We examined the possibility of aberrant expression of ADAM proteins in $Ace^{-/-}$ mouse sperm, as was noted for $Clgn^{-/-}$ sperm (shown in Fig. 1C) [12]. When the protein extract from $Ace^{-/-}$ testis was immunoprecipitated with the anti-CLGN antibody and the immunoprecipitate was subjected to immunoblot analysis using antibodies to ADAM1a, ADAM1b, ADAM2, and ADAM3, all of these ADAMs were detected (Fig. 3A). The $Ace^{-/-}$ testicular extract was also immunoprecipitated with the anti-ADAM2 antibody, and the precipitants were subjected to immunoblot analysis with the various anti-ADAM antibodies. Both ADAM1a and ADAM1b were detected in this immunoprecipitate, which suggests the formation of ADAM1a/ADAM2 and ADAM1b/ADAM2 heterodimers in the testis (Fig. 3B). Finally, the ADAMs were processed normally in $Ace^{-/-}$ sperm, which is similar to the situation observed in heterozygous sperm (Fig. 3C).

Aberrant Distribution of ADAM3 after Phase Separation of $Ace^{-/-}$ Sperm

Our results (Fig. 3) indicate that the ADAMs were present and processed normally in $Ace^{-/-}$ testes and sperm. The Triton X-114 phase separation method concentrates proteins into either a detergent-depleted or detergent-enriched phase, depending on the conformation of the protein [24]. When the proteins from $Ace^{-/-}$ sperm were fractionated into detergent-enriched and detergent-depleted phases with Triton X-114, most of the ADAM3 content (~80%) disappeared from the detergent-enriched phase, compared to the ADAM3 content of $Ace^{+/-}$ sperm (Fig. 4, A and B). In contrast, both the ADAM1b and ADAM2 levels remained the same in the detergent-enriched phases of the $Ace^{+/-}$ and $Ace^{-/-}$ sperm. We analyzed other sperm membrane proteins using this Triton X-114 phase separation system. Proteins that contain a transmembrane domain, e.g., IZUMO1 and CD46, were distributed in both phases, while the GPI-anchored SPAM1 (PH-20) protein was distributed exclusively in the detergent-enriched phase (Fig. 4A). Of the sperm proteins examined, only ADAM3 decreased in amount in the detergent-enriched phase of the $Ace^{-/-}$ sperm.

Comparison of Zona Pellucida-Binding Abilities for Clgn and Ace-Null Mouse Sperm

While aberrant subcellular distribution of ADAM3 was observed in both $Clgn^{-/-}$ and $Ace^{-/-}$ sperm, the altered localization was less severe in $Ace^{-/-}$ sperm (Fig. 4). To examine whether the sperm from these null animals differ in their zona pellucida-binding activities, the numbers of sperm bound per cumulus-free egg were determined. Both $Clgn^{-/-}$ and $Ace^{-/-}$ sperm bound eggs poorly, as compared to the wild-type sperm (Fig. 5B). Furthermore, eggs bound significantly lower numbers of $Clgn^{-/-}$ sperm than $Ace^{-/-}$ sperm ($P < 0.001$). These effects were not caused by differences in sperm motility, which remained normal in both knockout mouse lines [8, 16].

DISCUSSION

Although a number of proteins have been hypothesized to be essential for various events of fertilization, their actual roles when a particular gene was ablated were not clear [2–6]. The ADAM1b/ADAM2 dimer (fertilin) was initially thought to be involved in sperm-egg fusion [25] but was later postulated to be involved in the sperm–ZP interaction [7, 26]. More recently, ADAM1a/ADAM2 has been hypothesized to have a chaperone activity, serving to direct ADAM3 to the sperm membrane [10, 23]. Given that ablation of the *Adam3* gene impairs sperm–ZP binding [11], our findings suggest that ADAM3 acts downstream of the ADAMs network in sperm assembly and functions in sperm–zona pellucida binding.

In studying the aberrant zona pellucida-binding activity of $Ace^{-/-}$ sperm, we examined the integrity of ADAMs on these sperm compared with the $Clgn^{-/-}$ sperm [8]. We have previously reported the disappearance of ADAM2 from $Clgn^{-/-}$ sperm, and in the present study, we found that ADAM3 was also absent in $Clgn^{-/-}$ sperm (Fig. 1C). This loss of ADAM3 was more complete than that reported for $Adam2^{-/-}$ sperm, in which the ADAM3 level decreased to ~11% of the wild-type level [27]. In any case, if the loss of ADAM3 is caused by disruption of ADAM2, it was reasonable to assume that the ablation of both *Adam2* and *Adam3* would lead to a similar phenotype. In the same context, the impaired zona pellucida-binding activity of $Clgn^{-/-}$ sperm could be explained by an initial failure to form the ADAM1a/ADAM2 dimer, which led, as a secondary effect, to the disappearance of ADAM3 from the sperm surface. This scheme may explain why the four different gene knockout mouse lines (*Clgn*, *Adam1a*, *Adam2*, and *Adam3*) share a similar fertilization phenotype.

The impaired zona pellucida-binding activity of $Ace^{-/-}$ sperm cannot be explained by a similar mechanism, which raises the question as to how the disruption of *Ace* leads to a failure of sperm binding to the zona pellucida (Fig. 6). Although rodent tACE has been reported to localize to the midpiece of the sperm flagellum and then disappear from mature sperm during passage through the epididymis [28], we show that tACE is localized exclusively to the head of the sperm from the cauda epididymis, which suggests that tACE is involved in sperm-zona pellucida interactions. Recently, the GPIase activity of ACE has been reported to be necessary for the sperm to acquire ZP-binding activity [29]. Kondoh et al. have postulated that some GPI-anchored proteins on the sperm surface play roles in ZP interaction after cleavage or that tACE exposes a ZP-binding factor by shedding GPI-anchored proteins that block binding.

The appearance and localization of ACE was not affected in $Clgn^{-/-}$ sperm, which suggests that tACE is not a direct mediator of sperm-zona pellucida binding. Rather, we postulate that tACE is involved in distributing ADAM3 to a location in which it can participate in sperm-ZP binding. When ACE was missing, a portion of the ADAM3 content was not distributed in the detergent-enriched fraction of the *Ace*-deficient sperm (Fig. 6). All of the sperm ADAM3 is located on the plasma membrane [30, 31]. These reports and our findings indicate that some of the membranous ADAM3 content is distributed in the detergent-depleted fraction. Although the amount of ADAM3 in the detergent-enriched phase is small compared to the total amount, the lack of ADAM3 in this phase may have a detrimental effect on sperm function. The manner in which ACE affects ADAM3 distribution in sperm remains unknown, although the appropriate subcellular distribution of ADAM3 appears to be critical for the sperm to develop the ability to bind to the zona pellucida. Our experiments also suggest one

possible mechanism for the similar phenotypes observed when the genes for *Ace*, *Clgn*, *Adam1a*, *Adam2*, and *Adam3* were ablated, i.e., the disruption of zona pellucida-binding ability in these mouse lines is mediated entirely through the aberrant distribution of ADAM3. Recently, it has been reported that ADAM3 has zona-binding activity, while ADAM2 and SPAM1 do not have this activity [32]. This report reinforces the idea that ADAM3 is the furthest downstream factor in sperm-zona pellucida binding. Further study is needed to clarify whether ADAM3 participates in a direct or indirect manner in this process.

ACKNOWLEDGMENTS

We are grateful to Dr. Hitoshi Nishimura and Dr. Tadashi Baba (University of Tsukuba) for providing antibodies against SPAM1, ADAM1a, and ADAM1b and for helpful comments. We also thank Dr. Paul Primakoff (University of California, Davis) for providing the antibody against SPAM1.

REFERENCES

1. Nichols J, Gardner RL. Effect of damage to the zona pellucida on development of preimplantation embryos in the mouse. Hum Reprod 1989; 4:180–187.
2. Baba T, Azuma S, Kashiwabara S, Toyoda Y. Sperm from mice carrying a targeted mutation of the acrosin gene can penetrate the oocyte zona pellucida and effect fertilization. J Biol Chem 1994; 269:31845–31849.
3. Lu Q, Hasty P, Shur BD. Targeted mutation in beta1,4-galactosyltransferase leads to pituitary insufficiency and neonatal lethality. Dev Biol 1997; 181:257–267.
4. Baba D, Kashiwabara S, Honda A, Yamagata K, Wu Q, Ikawa M, Okabe M, Baba T. Mouse sperm lacking cell surface hyaluronidase PH-20 can pass through the layer of cumulus cells and fertilize the egg. J Biol Chem 2002; 277:30310–30314.
5. Ensslin MA, Shur BD. Identification of mouse sperm SED1, a bimotif EGF repeat and discoidin-domain protein involved in sperm-egg binding. Cell 2003; 114:405–417.
6. Inoue N, Ikawa M, Nakanishi T, Matsumoto M, Nomura M, Seya T, Okabe M. Disruption of mouse CD46 causes an accelerated spontaneous acrosome reaction in sperm. Mol Cell Biol 2003; 23:2614–2622.
7. Cho C, Bunch DO, Faure JE, Goulding EH, Eddy EM, Primakoff P, Myles DG. Fertilization defects in sperm from mice lacking fertilin beta. Science 1998; 281:1857–1859.
8. Ikawa M, Wada I, Kominami K, Watanabe D, Toshimori K, Nishimune Y, Okabe M. The putative chaperone calmegin is required for sperm fertility. Nature 1997; 387:607–611.
9. Krege JH, John SW, Langenbach LL, Hodgin JB, Hagaman JR, Bachman ES, Jennette JC, O'Brien DA, Smithies O. Male-female differences in fertility and blood pressure in ACE-deficient mice. Nature 1995; 375:146–148.
10. Nishimura H, Kim E, Nakanishi T, Baba T. Possible function of the ADAM1a/ADAM2 Fertilin complex in the appearance of ADAM3 on the sperm surface. J Biol Chem 2004; 279:34957–34962.
11. Shamsadin R, Adham IM, Nayernia K, Heinlein UA, Oberwinkler H, Engel W. Male mice deficient for germ-cell cyritestin are infertile. Biol Reprod 1999; 61:1445–1451.
12. Ikawa M, Nakanishi T, Yamada S, Wada I, Kominami K, Tanaka H, Nozaki M, Nishimune Y, Okabe M. Calmegin is required for fertilin alpha/beta heterodimerization and sperm fertility. Dev Biol 2001; 240: 254–261.
13. Kim E, Nishimura H, Baba T. Differential localization of ADAM1a and ADAM1b in the endoplasmic reticulum of testicular germ cells and on the surface of epididymal sperm. Biochem Biophys Res Commun 2003; 304: 313–319.
14. Nishimura H, Kim E, Fujimori T, Kashiwabara S, Kuroiwa A, Matsuda Y, Baba T. The ADAM1a and ADAM1b genes, instead of the ADAM1 (fertilin alpha) gene, are localized on mouse chromosome 5. Gene 2002; 291:67–76.
15. Hubert C, Houot AM, Corvol P, Soubrier F. Structure of the angiotensin I-converting enzyme gene. Two alternate promoters correspond to evolutionary steps of a duplicated gene. J Biol Chem 1991; 266:15377–15383.
16. Hagaman JR, Moyer JS, Bachman ES, Sibony M, Magyar PL, Welch JE, Smithies O, Krege JH, O'Brien DA. Angiotensin-converting enzyme and male fertility. Proc Natl Acad Sci U S A 1998; 95:2552–2557.
17. Kessler SP, Rowe TM, Gomos JB, Kessler PM, Sen GC. Physiological non-equivalence of the two isoforms of angiotensin-converting enzyme. J Biol Chem 2000; 275:26259–26264.
18. Ramaraj P, Kessler SP, Colmenares C, Sen GC. Selective restoration of male fertility in mice lacking angiotensin-converting enzymes by sperm-specific expression of the testicular isozyme. J Clin Invest 1998; 102:371–378.
19. Lin Y, Mahan K, Lathrop WF, Myles DG, Primakoff P. A hyaluronidase activity of the sperm plasma membrane protein PH-20 enables sperm to penetrate the cumulus cell layer surrounding the egg. J Cell Biol 1994; 125:1157–1163.
20. Inoue N, Ikawa M, Isotani A, Okabe M. The immunoglobulin superfamily protein Izumo is required for sperm to fuse with eggs. Nature 2005; 434: 234–238.
21. Bordier C. Phase separation of integral membrane proteins in Triton X-114 solution. J Biol Chem 1981; 256:1604–1607.
22. Toyoda Y, Yokoyama M, Hoshi T. Studies on the fertilization of mouse egg in vitro. Jpn J Anim Reprod 1971; 16:147–151.
23. Stein KK, Go JC, Primakoff P, Myles DG. Defects in secretory pathway trafficking during sperm development in adam2 knockout mice. Biol Reprod 2005; 73:1032–1038.
24. Florke RR, Schnaith K, Passlack W, Wichert M, Kuehn L, Fabry M, Federwisch M, Reinauer H. Hormone-triggered conformational changes within the insulin-receptor ectodomain: requirement for transmembrane anchors. Biochem J 2001; 360:189–198.
25. Blobel CP, Wolfsberg TG, Turck CW, Myles DG, Primakoff P, White JM. A potential fusion peptide and an integrin ligand domain in a protein active in sperm-egg fusion. Nature 1992; 356:248–252.
26. Yamagata K, Nakanishi T, Ikawa M, Yamaguchi R, Moss SB, Okabe M. Sperm from the calmegin-deficient mouse have normal abilities for binding and fusion to the egg plasma membrane. Dev Biol 2002; 250:348–357.
27. Nishimura H, Cho C, Branciforte DR, Myles DG, Primakoff P. Analysis of loss of adhesive function in sperm lacking cyritestin or fertilin beta. Dev Biol 2001; 233:204–213.
28. Metayer S, Dacheux F, Dacheux JL, Gatti JL. Germinal angiotensin I-converting enzyme is totally shed from the rodent sperm membrane during epididymal maturation. Biol Reprod 2002; 67:1763–1767.
29. Kondoh G, Tojo H, Nakatani Y, Komazawa N, Murata C, Yamagata K, Maeda Y, Kinoshita T, Okabe M, Taguchi R, Takeda J. Angiotensin-converting enzyme is a GPI-anchored protein releasing factor crucial for fertilization. Nat Med 2005; 11:160–166.
30. Kim E, Nishimura H, Iwase S, Yamagata K, Kashiwabara S, Baba T. Synthesis, processing, and subcellular localization of mouse ADAM3 during spermatogenesis and epididymal sperm transport. J Reprod Dev 2004; 50:571–578.
31. Kim T, Oh J, Woo JM, Choi E, Im SH, Yoo YJ, Kim do H, Nishimura H, Cho C. Expression and relationship of male reproductive ADAMs in mouse. Biol Reprod 2006; 74:744–750.
32. Kim E, Baba D, Kimura M, Yamashita M, Kashiwabara S, Baba T. Identification of a hyaluronidase, Hyal5, involved in penetration of mouse sperm through cumulus mass. Proc Natl Acad Sci U S A 2005; 102: 18028–18033.

配偶子形成から受精まで

6．受精のメカニズム

—イズモを中心に卵子と精子の結合に必要な因子とその異常に関連した受精異常について—

井上直和*・伊川正人*・岡部 勝*
大阪大学微生物病研究所附属遺伝情報実験センター．

Key Words/ノックアウトマウス，受精，膜融合

要旨

ほ乳類の受精に重要な因子が遺伝子ノックアウトにより次々と同定されてきている．ノックアウトマウスを用いた解析の特徴は，その表現型から，受精に必要な分子かどうかの判定が明確にくだされることである．長い受精研究の歴史のなかで重要であるとされた因子であっても，実は不要であると判明することがあれば，逆にまったく想像されていなかった分子が重要な場合もある．本稿では，遺伝子ノックアウトから得られた解析結果を中心に，受精の各現象と，それに寄与する分子について解説する．

はじめに

これまでのほ乳類の受精現象についての研究は，形態学的な観察や生理学的な解析が中心となって発展してきたが，近年，遺伝子組換えマウスを用いた研究が可能になったことで，これまでの解析により明らかにされてきた情報をもとに，ノックアウトマウスを作製し，分子生物学的な解析がなされるようになった．その結果，さまざまな不妊モデルマウスが作製され，それらの精子，卵子の動態を観察することで受精の各ステップにかかわる重要な因子が浮き彫りになってきている．これら因子のなかには，以前には知られなかった「意外な」因子も報告され，新しい展開もある．本稿では，混沌の中からおぼろげに現れようとしている新しい受精の分子メカニズムを紹介したい．

受精とは？

受精は，射出された多くの精子（ヒトの場合1～3億匹）のなかで，最終的にたった一匹の精子が卵子と融合し，遺伝情報を受け渡す過程である．射出された精子には受精に至るまでにさまざまな障害が立ちはだかり，優れた精子が選択を受けているようにもみえる．本稿では卵

0386-9792/06/¥100/頁/JCLS

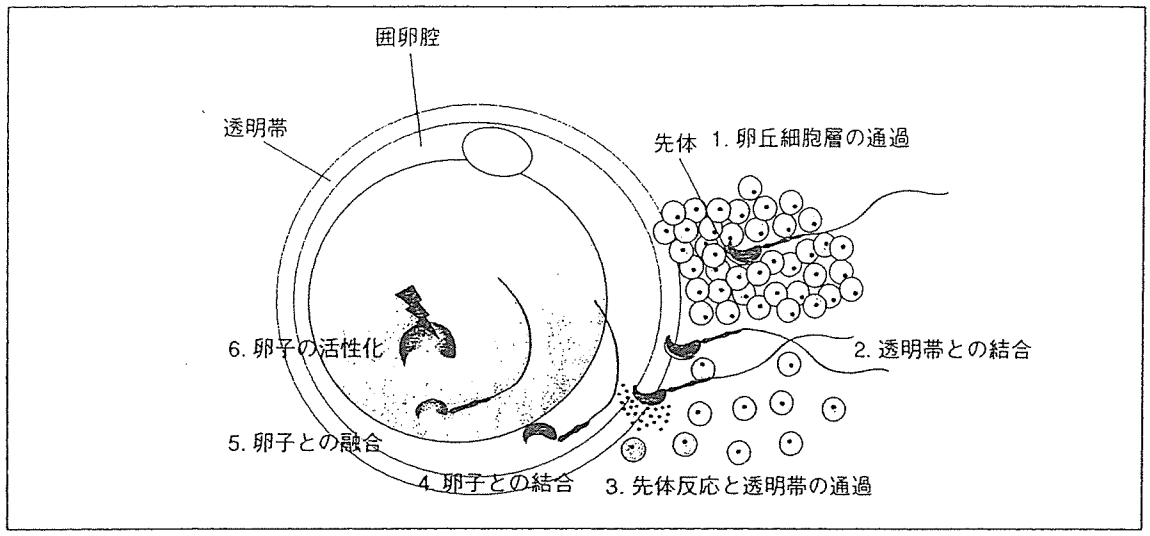

図1 マウスにおける受精メカニズム

マウスの精子は輸卵管に移行後，1. 卵丘細胞層の通過，2. 透明帯との結合，3. 先体反応と透明帯の通過，4. 卵子との結合，5. 卵子との融合，5. 卵子の活性化を経て受精が完了する．

管膨大部に到達した精子が卵丘細胞を通過し，卵子と融合するまでの分子機構を紹介したい．また，受精のメカニズムは種によって少しずつ異なっているので，ここではマウスをモデルとして話を進める．

図1に示すように，受精に至るまでのステップはいくつかに分けることができる．卵管内を上昇してきた精子は卵管膨大部において卵子を取り囲んでいる卵丘細胞層と出会う．精子はヒアルロン酸で架橋された卵丘細胞間の間隙を通り抜け，卵子の周りを取り囲んでいる糖蛋白質の層である透明帯に結合し，透明帯からの刺激により先体反応と呼ばれる形態的変化を起こす．さらに，精子は先体内の加水分解酵素により透明帯を分解しながら通過した後，卵細胞膜と結合し，融合する．こうして精子は，染色体を卵子に送り込むと同時に卵子を活性化してはじめて受精が成立する．

卵丘細胞層の通過

卵丘細胞層は卵丘細胞同士がヒアルロン酸を主とするマトリックスで弱く結合しており，精子はヒアルロン酸分解酵素を用いながらこの層を通過すると考えられている．精子に存在するPH-20は，ハチ毒に含まれるヒアルロニダーゼと類似するため精子の卵丘細胞の通過に必要な因子と考えられてきた．しかし，この分子をノックアウトしても精子はマトリックスを通過し受精することができるうえに，精子にはHyal5と呼ばれる新たなヒアルロニダーゼも存在していた[1)2)]．PH20の機能をHyal5が補う可能性も考えられるため，Hyal5のみならずPH20とのダブルノックアウトマウスの解析結果が待たれる．

透明帯への結合

1. 透明帯の形成因子

卵子は透明帯と呼ばれる細胞外マトリックスにより覆われているが，透明帯はおもにZPA, ZPB, ZPCの三種類の糖蛋白質から成っている．マウスの場合，精子との相互作用には少なくとも2段階あり，先体反応を起こす前の精子

細胞膜と結合する最初のレセプターがZPC（ZP3）であり，先体反応後の先体内膜に結合するセカンドレセプターがZPA（ZP2）であると考えられている．また，ZP3のO結合型糖鎖が精子との相互作用に重要である．ZP3のノックアウトマウスの卵子は透明帯を形成できないために脆弱で受精能がないが，ヒトZP3分子を発現させることにより透明帯が再構築し，受精能が回復する[3]．さらに，ZP2をヒト型に置換した場合でもマウス精子が透明帯に結合，通過できる．しかし，これらの透明帯とヒト精子は相互作用を示さないことから，透明帯因子の糖鎖の構造が種特異性を決定していると推測される．

2．透明帯結合に関わる雄側の因子

精子が透明帯に結合できなくなるようなノックアウトマウスはいくつか報告されているが，どの分子も直接の透明帯結合因子とはいいがたく，混沌とした状況にある．

1）カルメジン

カルメジンは精細胞の分化時期に特異的に発現し，体細胞の小胞体に存在するカルネキシンによく似た因子で，レクチン型の分子シャペロンである．カルメジンノックアウトの雌はまったく正常であるが，雄は見かけ上は正常であり，交尾して射精に至るにもかかわらず不妊であった．さらに，その精子は形態や運動性に異常は見つからなかったが，透明帯にまったく結合できないことが判明した[4]（図2-a）．カルメジンは精巣内でのみ発現し，成熟精子上からは消失する蛋白質であることから，精子上で透明帯との結合に直接作用しているとは考えにくく，カルメジンによって折りたたまれる精子上の因子が透明帯との結合に関与していることが予想される．

2）ADAM（A Disintegrin And Metalloprotease）ファミリー

受精の相互作用に関する膜型蛋白質として，ファーティリン（ADAM1bとADAM2のヘテロダイマー）やシリテスティン（ADAM3）などのADAMファミリーが見い出された．精細胞ではADAM1a，ADAM1b，ADAM2，ADAM3が発現し，ADAM1aとADAM2，

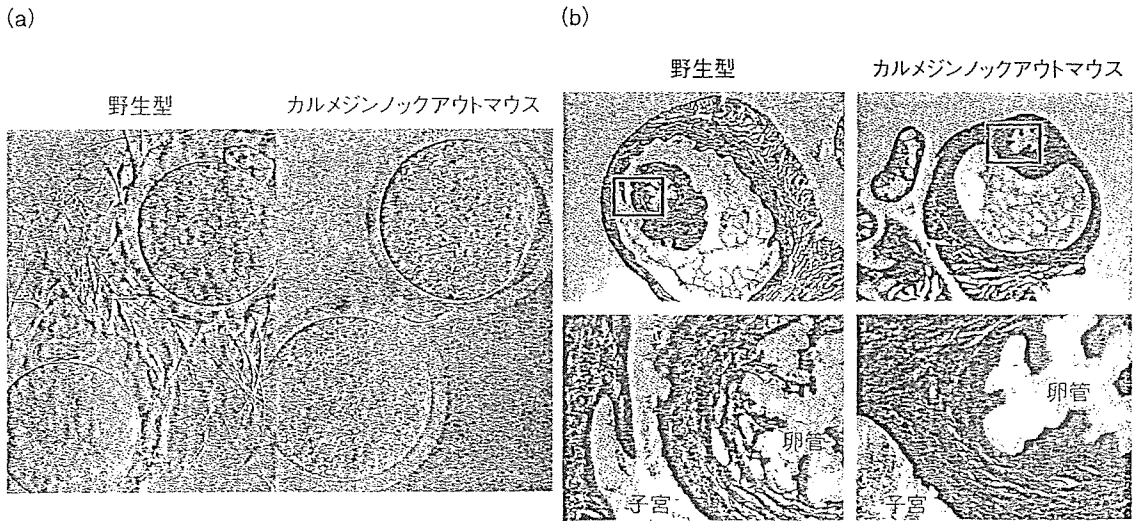

図2　カルメジンノックアウトマウスの精子は透明帯への結合と輸卵管への移行が損なわれる

(a) カルメジンノックアウトの精子はまったく透明帯に結合することができないため，不妊になる．(b) 射精後，カルメジンノックアウトの精子は卵管内に全く観察されず，子宮―卵管接合部まで到達できないことが分かる．（文献4，9より改変・転載）

表1 カルメジンおよびADAMファミリーのノックアウトマウスの表現型

genotype	Testicular moleules		Sperm molecules			zona binding	UTJ migration
	Calmegin	ADAM1a	ADAM1b	ADAM2	ADAM3		
Calmegin-KO	×	n.d.	×	×	×	impaired	impaired
ADAM1a-KO	○	×	○	○	△	impaired	impaired
ADAM1b-KO	○	○	×	○	○	normal	normal
ADAM2-KO	n.d.	○	×	×	△	impaired	impaired
ADAM3-KO	n.d.	○	○	○	×	impaired	normal

○: present, ×: absent, △: reduced n.d.: no data

ADAM1bとADAM2はヘテロダイマーを形成する．ADAMファミリー蛋白質は，メタロプロテアーゼドメイン，ディスインテグリンドメイン，システインリッチドメイン，EGF様リピートドメインなど，多様なドメイン構造をもつ．とくにADAM1bは，ウイルスの融合ペプチドと相同性のある配列を有しているため，卵子との融合に重要な蛋白質であると最初は考えられていたが，ADAM1bノックアウトマウスの雄が不妊にならないことからこの仮説は覆された[5]．ところが，ADAM1a，ADAM2，ADAM3ノックアウトマウスの雄は不妊になり，その精子は共通に透明帯への結合能が損なわれることが示された[6)~8)]．さらに，ADAM1a，ADAM2をそれぞれノックアウトすると，精子上のADAM3が減少することが判明した．このため，これらの分子はお互いに非常に密接な関係にある(表1)．

さらに興味深いことに，カルメジンノックアウトマウスの精子ではファーティリンやADAM3が精子からなくなっていた[9]．

3) アンジオテンシン変換酵素 (ACE)

ACEは，血液中のアンジオテンシンⅠやブラジキニンといったペプチドのC末端の2アミノ酸を遊離させる酵素活性を有し，血圧の調節に関与する分子であるが，イントロン12に存在する精巣特異的なプロモーターによって，分子量の小さい精巣型ACEも産生される．ACEをノックアウトすると，血圧低下が起こると同時に，その精子が透明帯と結合できなくなり，不妊となる[10]．体細胞型のACEだけを欠損した精子が受精能を有していることや，精巣型ACEをノックアウトマウスに発現させると受精能が回復することから，透明帯の結合には精巣型ACEが深く関与している．精巣型ACEが直接のレセプターとして透明帯に相互作用するのか，あるいは，その酵素作用が精子上の因子を修飾して透明帯結合に作用するのかについては不明であったが，最近，ACEにはジペプチジルカルボキシペプチダーゼ活性の他にGPIアンカー型蛋白質を切断する活性があることが報告された[11]．さらに，ACEのペプチダーゼ活性中心のアミノ酸を変異させたリコンビナント蛋白質を，*in vitro*でACEノックアウト精子に加えても透明帯への結合能力が回復したことから，ACEのGPIアーゼ活性が透明帯との結合に重要な働きをしており，そのターゲットとなるGPIアンカー型蛋白質が透明帯への結合に深く関与していることが推測される．今後の研究の進展によっては，透明帯への結合の詳細な分子メカニズムの解明に繋がるであろう．

今回はノックアウトによって証明された透明帯結合因子を紹介したが，このほかにもSp56，zonadhesinなど，未だノックアウトされていない分子を含めると候補分子はその数を増やしているが，現時点ではお互いの関連性は十分に分かっていない．また，カルメジン，ACE，ADAM1a，ADAM2のノックアウトでは輸卵管内に精子が昇っていかないという別の表現型が

共通に存在することも知られており（図2-b），今後は，透明帯への結合と輸卵管内への移行がなぜ相関しているのかを明らかにするとともに，これらのノックアウトマウスにおそらく共通して機能が損なわれている真の透明帯結合因子を同定する必要がある．

先体反応

一般に，受精能を獲得した精子は透明帯に結合した後，透明帯の刺激により先体反応を起こし透明帯を通過する，といわれている．先体反応は，精子先体部分の膜構造がなくなり，先体内の蛋白質を放出する精子の構造変化を伴う反応である．先体反応を起こしていない精子は融合できないことから，先体反応は受精にとって必須な現象である．精子を活性化する透明帯の活性成分としてはZP3が有名であるが，その他の物質による先体反応の誘導についても多くの報告がある．しかし，いずれのメカニズムを経るにせよ先体反応には精子細胞外からのCa^{2+}の流入が必要である．

精子内へのCa^{2+}の流入に伴い，惹起される先体反応には，細胞膜上のイノシトール1,4,5-トリスリン酸（PI_3）のシグナルが必要と思われていたが，その実体は明らかではなかった．そのようななかで，精巣特異的に発現するPLCδ

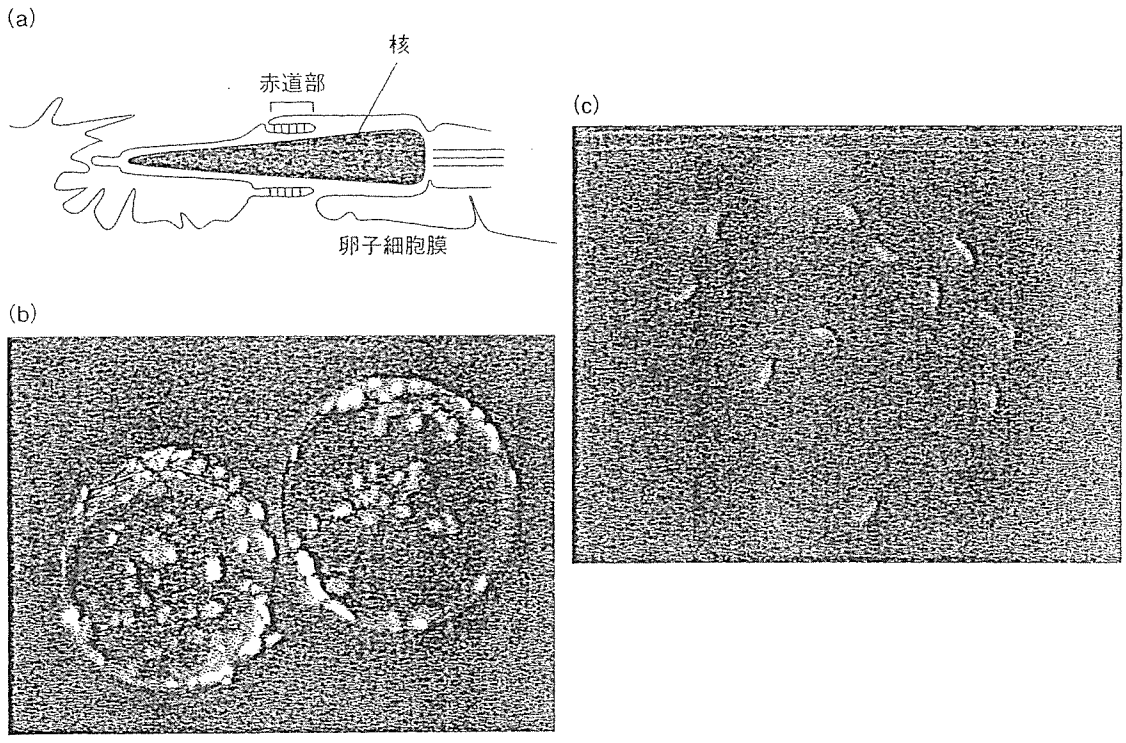

図3 融合能欠損を示すCD9ノックアウト卵子とIzumoノックアウト精子

(a) 精子/卵子の膜融合は精子側の赤道部から始まる．(b) CD9ノックアウト卵子に対して精子を加えヘキスト33342で精子の核を染色すると，精子は正常に透明帯を通過するが，融合できないため囲卵腔に蓄積されている様子が観察される．(c) Izumoノックアウト精子は先体反応を引き起こし，透明帯を通過することができるが，融合がまったく起こらないため囲卵腔に精子が多数存在する．なお，先体反応の有無は，先体反応後の精子に特異的に反応する抗体MN9（千葉大学の年森清隆教授よりご供与いただいた）を用いて染色し評価した．

4 (Phospholipase Cδ4) のノックアウトマウスが作製され，その精子は可溶化した透明帯にさらしてもほとんど先体反応を起こさないことから，PLC δ4 を介した PI_3 のシグナルが先体反応にとって重要な働きをすることが明らかになった[12]．

卵子との融合

先体反応を終えた精子は，速やかに卵子の細胞膜と結合し融合を開始する．ヒトを含む真獣類では先体赤道部の細胞膜で融合し始める（図3-a)．この部分は精子が先体反応を起こす前から表面に露出しているが，不思議なことに先体反応前に精子が卵子と融合することはない．

これまでに，生化学的な解析から精子のファーティリンや卵子のインテグリン $\alpha 6 \beta 1$ が，融合因子と考えられていた時期があったが，これらの分子をノックアウトしても融合能に大きな変化が認められないことから，これら因子の重要性は疑問視されている．

1. 卵子上の融合因子

1) テトラスパニン

4回膜貫通型のファミリー分子（テトラスパニン）であるCD9をノックアウトすると雌マウスは不妊になるが，その原因は透明帯通過後の精子が卵子と融合できないためである（図3-b)．CD9ノックアウト卵子でも顕微授精により精子を細胞質内に直接注入すると，正常に産仔が得られることから，この分子が融合のステップに特異的に関与していることが証明された[13]．さらに，最近になって同じテトラスパニンのCD81のノックアウトの雌も妊孕性が低下し，その卵子もほとんど融合できなくなることが報告された[14]．この論文のなかで合わせて，CD9は融合時に卵子細胞膜から精子の頭部に移動する像が観察された．この現象が真実であるならば，CD9はいつ，どのように精子頭部に移動し，融合に対してはどのような意味があるのか非常に興味が持たれるところである．

2) GPIアンカー型蛋白質

GPIアンカーの生合成系に重要なPig-aを，卵子特異的なZP3プロモーターを用いたCre-LoxPシステムによりコンディショナルノックアウトすると，その卵子は，精子と結合できるものの融合能がほとんど失われた[15]．このことから，卵子上のGPIアンカー型蛋白質が融合に関与することが考えられるが，卵子上のすべてのGPIアンカー型蛋白質を欠失させたことによる膜構造変化など2次的要因に起因する可能性も否めない．融合に寄与する特定のGPIアンカー型蛋白質を同定することを含め，今後，詳細な解析が必要とされる．

2. 精子上の融合因子

1) Izumo

卵子との融合を阻害する抗精子抗体（OBF13）の抗原として同定されたIzumo蛋白質は，縁結びの神様がいる出雲大社に因んで名付けられた．Izumoは免疫グロブリンスーパーファミリーに属し，細胞外に免疫グロブリン様ドメインをひとつだけもつI型の膜貫通型蛋白質である．Izumoは射精直後の精子膜表面にはなく，先体反応を起こした精子において，はじめて膜表面に露出し，赤道部を含む頭部全体に分布する．

Izumoをノックアウトすると，雌は正常であるが雄マウスは交配しても妊孕性を示さず，その精子は，卵子と融合する能力を完全に欠失していることがわかった（図3-c)．Izumoが融合の過程に特異的に作用する分子であることは，Izumoノックアウト精子が透明帯を正常に通過し，卵子細胞膜と結合能を保持することのほかに，顕微授精法で融合ステップをバイパスさせるとノックアウト精子からも産仔を得ることができることで示された．また，特異的抗体を用いた受精阻害実験から，ヒトIzumoも卵子との